AUTOPHAGY
2022, VOL. 18, NO. 12, 3004–3022
https://doi.org/10.1080/15548627.2022.2056864

Taylor & Francis
Taylor & Francis Group

TOOLBOX

OPEN ACCESS Check for updates

An optimized protocol for immuno-electron microscopy of endogenous LC3

Ann De Mazière [a], Jan van der Beek [a], Suzanne van Dijk[a], Cecilia de Heus [a], Fulvio Reggiori [b], Masato Koike [c], and Judith Klumperman [a]

[a]Section Cell Biology, Center for Molecular Medicine, University Medical Center Utrecht, Utrecht University, Utrecht, The Netherlands; [b]Department of Biomedical Sciences of Cells & Systems, University of Groningen, University Medical Center Groningen, Groningen, The Netherlands; [c]Department of Cell Biology and Neuroscience, Juntendo University Graduate School of Medicine, Tokyo, Japan

ABSTRACT

MAP1LC3/LC3 (microtubule associated protein 1 light chain 3) is widely used as marker of autophagic compartments at different stages of maturation. Electron microscopy (EM) combined with immunolabeling is the only technique that can reveal the ultrastructural identity of LC3-labeled compartments. However, immuno-EM of endogenous LC3 proteins has proven difficult. Here, we test a panel of commercially available antibodies and apply different labeling conditions to present an optimized procedure for LC3 immuno-EM. Using ultrathin cryosections and protein A-colloidal gold or gold enhancement labeling, we localize endogenous LC3 in starved cells or tissues in the presence or absence of the proton pump inhibitor bafilomycin A_1. We localize LC3 to early and late stage autophagic compartments that can be classified by their morphology. By on-section correlative light-electron microscopy (CLEM) we show that comparable fluorescent LC3-positive puncta can represent different autophagic intermediates. We also show that our approach is sufficiently robust to label endogenous LC3 simultaneously with other lysosomal and autophagy markers, LAMP1 or SQSTM1/p62, and can be used for quantitative approaches. Thus, we demonstrate that bafilomycin A_1 treatment from 2.5 up to 24 h does not inhibit fusion between autophagosomes and lysosomes, but leads to the accumulation of LC3-positive material inside autolysosomes. Together, this is the first study presenting an extensive overview of endogenous LC3 localization at ultrastructural resolution without the need for cell permeabilization and using a commercially available antibody. This provides researchers with a tool to study canonical and non-canonical roles of LC3 in native conditions.

ARTICLE HISTORY
Received 18 August 2021
Revised 11 March 2022
Accepted 15 March 2022

KEYWORDS
Autophagy; bafilomycin A1; CLEM; immuno-electron microscopy; LC3; ultrathin cryosections

Introduction

Macroautophagy (hereafter called autophagy) is a process by which cells recycle cytosolic components and organelles by delivering them to lysosomes [1–8]. Autophagy begins with the enclosure of a portion of the cytoplasm by a cup-shaped cisterna, the phagophore, which expands and fuses at the extremities to become a closed, double-membrane structure called an autophagosome. Autophagosomes can fuse with late endosomes resulting in the formation of amphisomes, which then fuse with lysosomes to form autolysosomes. Alternatively, autophagosomes fuse directly with lysosomes [9]. In autolysosomes, the low pH and the presence of hydrolytic enzymes result in the breakdown of the autophagic cargo. In case this process is blocked, such as when using the vacuolar type H^+-ATPase (V-ATPase) inhibitor bafilomycin A_1 (BafA1), autophagocytosed cargo remains visible as autophagic content within the autolysosomal lumen (see Figure 1A for a schematic representation of the different endo-lysosomal and autophagic compartments). Autophagy is important for the generation of metabolites that can be re-used for *de novo* biosynthesis of macromolecules or energy production.

The formation of the phagophore and its elongation and closure to generate an autophagosome are mediated by autophagy-related (ATG) proteins [10]. Upon induction of autophagy, a serine/threonine kinase complex (ULK1 or ULK2, ATG13, RB1CC1/FIP200, ATG101) is activated, which together with an autophagy-specific phosphatidylinositol-3 kinase (PtdIns3K) complex (PIK3C3/VPS34, ATG14, BECN1, PIK3R4/VPS15, NRBF2) and ATG9A-positive membranes initiates the formation of the phagophore (see Figure 1A, [11]). The local production of phosphatidylinositol-3-phosphate (PtdIns3P) by the PtdIns3K complex allows the recruitment of other ATG proteins important for the expansion of the phagophore, such as WIPI2 and ATG2A/ATG2B. Phagophores often form in specialized ER subdomains, known as omegasomes [12]. PtdIns3P is also required for the recruitment of two ubiquitination-like systems of ATG proteins, which transform cytosolic, non-lipidated LC3 proteins (LC3s; LC3-I) into lipidated LC3 (LC3-II). LC3-II through its conjugation to phosphatidylethanolamine becomes bound to the external and internal surfaces of the expanding phagophore, where it is required for the expansion and closure of the phagophore and binding of autophagic cargoes via the so-called autophagy receptors, such as SQSTM1/p62 [7, 13]. After closure of the phagophore, LC3-II is released from the outer membrane, but remains associated with the inner membrane. Subsequent fusion with late endosomes or lysosomes results in the merge of autophagosomal and lysosomal components and ultimately

CONTACT Judith Klumperman j.klumperman@umcutrecht.nl Section Cell Biology, Center for Molecular Medicine, University Medical Center Utrecht, Utrecht University, Utrecht, The Netherlands

Supplemental data for this article can be accessed here

© 2022 The Author(s). Published by Informa UK Limited, trading as Taylor & Francis Group.
This is an Open Access article distributed under the terms of the Creative Commons Attribution-NonCommercial-NoDerivatives License (http://creativecommons.org/licenses/by-nc-nd/4.0/), which permits non-commercial re-use, distribution, and reproduction in any medium, provided the original work is properly cited, and is not altered, transformed, or built upon in any way.

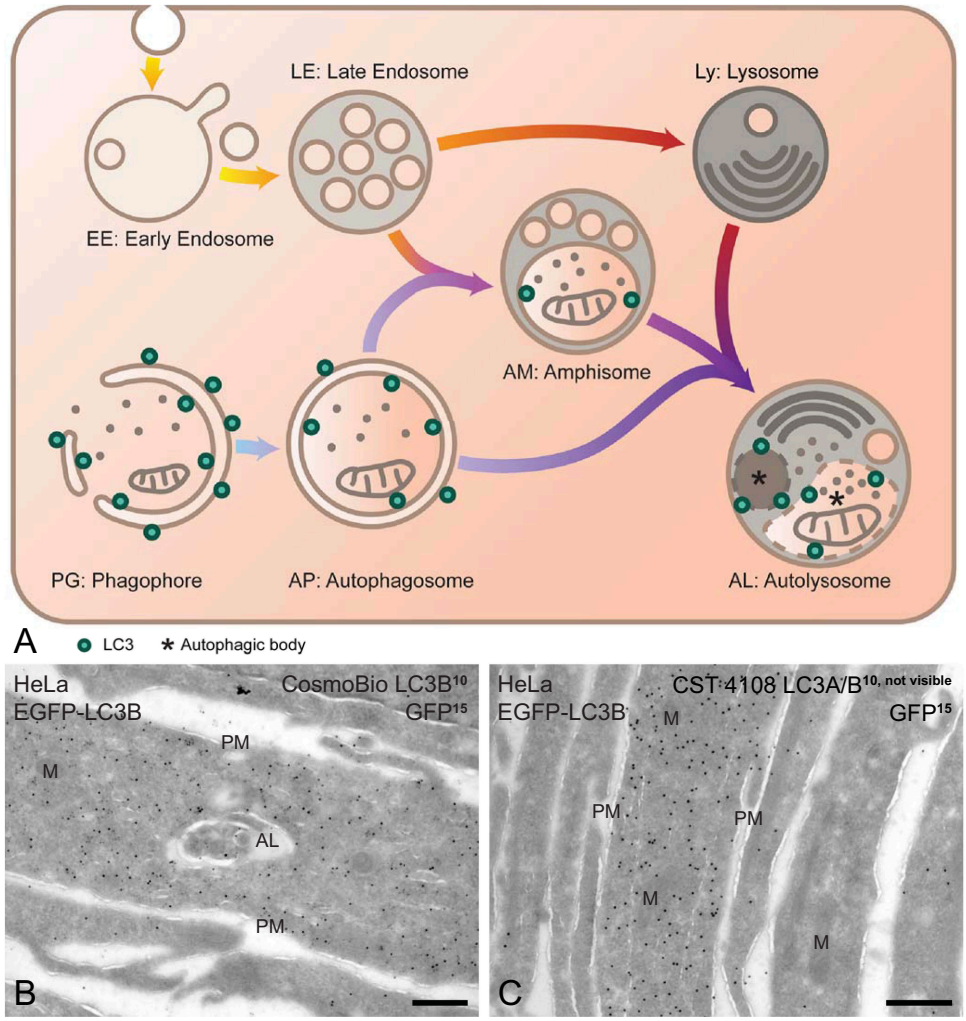

Figure 1. Cosmo Bio anti-LC3B specifically recognizes LC3B in EGFP-LC3B transfected cells. (A) Schematic overview of endo-lysosomal and autophagic compartments, outlining their characteristic morphological features and presence of LC3. (B-C) EGFP-LC3B transfected cells were fixed with 2% PFA+0.2% GA for 3 h and double labeled for LC3B and GFP and protein A gold (PAG). (B) The labeling intensities of anti-GFP (1:400; PAG15) and Cosmo Bio anti-LC3B (1:10; PAG10) correlate in cells with high and low EGFP-LC3B overexpression. (C) Example of double labeling with anti-GFP (1:400; PAG15) and another LC3 antibody (CST, 4108, 1:15; PAG10) showing only PAG15 on EGFP-LC3B overexpressing cells. AL, autolysosome; M, mitochondrion; PM, plasma membrane. Scale bars: 300 nm.

the formation of an autolysosome in which LC3-II and the sequestered cargo are degraded. Hence, LC3 is considered as marker protein for the phagophore and autophagosome, and, in some conditions, can be found in amphisomes and autolysosomes.

Fluorescence microscopy of immuno-labeled LC3, GFP-LC3 or mRFP-GFP-LC3 is a common method to study the occurrence of phagophores and autophagosomes in different conditions [14]. Expression of fluorescently tagged LC3s allows for live-cell imaging, but such exogenous expression can introduce artifacts [15] and is challenging to perform in tissues and specialized cell systems. Endogenous localization of LC3s is therefore an important tool to study autophagy in native conditions. A panel of commercial antibodies is available and routinely used in immunofluorescence (IF) and immunohistochemistry to localize endogenous LC3s [16–19]. While these antibodies cannot distinguish between LC3-I and LC3-II, it is generally assumed that a diffuse staining pattern represents cytosolic LC3-I, whereas a punctate pattern represents LC3-II associated with autophagosomal membranes [20, 21]. However, LC3-I can also be incorporated into cytoplasmic protein aggregates [15], and LC3-II can be recruited to non-autophagosomal membranes, such as for example to endosomes or lysosomes in the processes of endosomal microautophagy and lysosomal membrane repair [22–26], as well as to lipid droplets [27] and the plasma membrane [28]. Thus, LC3-positive puncta can represent different cellular structures [29].

Immuno-electron microscopy (immuno-EM) is the only microscopy method that reveals membranes and cellular context of immunolabeled proteins. Immuno-EM is therefore a key tool to classify LC3-labeled structures by their morphology, making it possible to identify the distinct stages of autophagy but also other organelles [9, 14, 30]. However, by conventional EM of plastic sections, the double-membrane of phagophores or autophagosomes cannot always be unequivocally distinguished from e.g. cell interdigitations or small mitochondria [31]. Also, the distinction between autophagosomes, amphisomes and autolysosomes is often difficult to make without the use of additional molecular markers. Hence,

Table 1. Performance of commercial LC3 antibodies in IF and immuno-EM.

				IF tests		Immuno-EM tests				
				4% PFA 20 min		4% PFA ON			2% PFA+0.2% GA 3 h	
Antibody*	LC3	Host	Test range**	GFP-LC3‡	Fig.	GFP-LC3†	Fig.	U2OS††	GFP-LC3†	U2OS††
Cosmo Bio	B	Ms	1:4–20 (1:10)	++	S1F	+++	1B	++	++	+
CST 4108	A/B	Rb	1:15–50	-	S1G	-	1C	nd	-	nd
CST 12741S	A/B	Ms	1:5–50	+	S1D	-	S2D	-	-	-
CST 2775	B	Rb	1:5–400	nd	nd	nd	nd	-	nd	-
MBL	A/B	Rb	1:2–100 (1:10)	+	S1B	±	S2B	±	-	-
Millipore	A	Rb	1:5–100	-	S1C	-	S2C	-	-	-
Nanotools	B	Ms	1:2–50	++	S1A	-	S2A	-	-	nd
Novus Biol.	B	Rb	1:2–250 (1:10)	+	S1E	±	S2E	±	±	nd
Sigma	A/B	Rb	1:5–200	nd	nd	nd	nd	-	nd	-

*Catalog numbers of tested antibodies: Cosmo Bio CAC-CTB-LC3-2-IC, MBL M152-3, Millipore MABC177, clone EP1528Y, Novus Biologicals NB600-1384, Nanotools 0231–100/LC3-5F10, Sigma L8918. ** Antibody dilution test range for immuno-EM, with optimal dilution in parentheses. ‡ IF staining of whole HeLa cells on coverslips, expressing EGFP-LC3B. † Starved HeLa cells with GFP-LC3B overexpression. †† U2OS cells starved in presence of BafA1, expressing endogenous LC3 only. LC3, LC3 isoform specificity; Ms, mouse; Rb, rabbit; nd, not determined. +++ = very strong labeling (e.g., Figure 1B); ++ = strong labeling (e.g. Figure 3, Figure 4A-C); + = significant staining (e.g. Figure 4D, Figure 5C, D); ± = just above background; – = no specific labeling; CST = Cell Signaling Technology.

an optimized protocol for LC3 localization by immuno-EM, which identifies the morphology of LC3-positive structures and allows for double-labeling with other relevant marker proteins, is highly warranted.

Detection of endogenous LC3 by immuno-EM has, however, proven difficult [14]. There are only few studies showing the localization of endogenous LC3 at the ultrastructural level and the methods used are limited in application. Pre-embedding immunogold labeling followed by silver or gold enhancement [20, 32, 33] yields a relatively high signal, but the need for membrane permeabilization leads to a loss of fine-structural integrity and the enhancement procedure prevents application of double labeling. Pre-embedding immuno-EM combined with horseradish peroxidase (HRP)-based labeling [34] results in a diffuse enzyme product with poor spatial resolution and also precludes double-labeling. Post-embedding immunogold labeling of methacrylate resin sections [35, 36] results in better morphology than pre-embedding labeling, but here the antigenicity of LC3 is severely affected by the embedding procedure, resulting in poor label yield.

The difficulties of the above-mentioned immuno-EM techniques are circumvented by immunogold labeling of ultrathin cryosections, also known as the Tokuyasu method. Here, labeling is performed after sectioning, which precludes the need for membrane permeabilization [37, 38]. Combined with the use of different-sized colloidal gold particles tagged to protein-A (PAG), this method allows for quantitative double labeling studies [39]. Although examples of endogenous LC3 labeling using this method have been shown [40–43], two major bottlenecks hamper broader implementation: appropriate preservation of the morphology of phagophore and autophagosomal membranes [14] and the availability of a commercial antibody that is sufficiently effective on cryosections. Generally, the fixation protocol for cryosections is very mild in order to preserve antigenicity. Preserving ultrastructure of phagophores and autophagosomes is then particularly challenging since these membranes contain only few transmembrane proteins [44], which hampers fixation by cross-linking agents as paraformaldehyde (PFA) and glutaraldehyde (GA). In order to maximize immuno-EM of LC3, the optimal balance between fixation and interaction between LC3 epitope and antibody has to be established. In this paper, we present an effective immuno-EM labeling protocol for endogenous LC3, using a commercially available antibody and with maximal preservation of ultrastructure. We believe this will provide a valuable tool for the large and fast-growing community of researchers studying autophagy in healthy and pathological situations.

Results

Selection of commercial LC3 antibodies for immuno-EM on cryosections

To find antibodies that perform optimally in LC3 immuno-EM, we acquired a panel of commercially available antibodies (Table 1) raised against one or more isoforms of LC3 [16–18]. Among the LC3s, LC3B is the most widely expressed and studied isoform. We therefore tested the commercial antibodies in transiently transfected HeLa cells overexpressing enhanced green fluorescent protein (EGFP)-LC3B. This ensured the presence of sufficient levels of LC3B and allowed us to directly compare the signal obtained by anti-LC3 antibodies with GFP fluorescence, using GFP as positive control for LC3B expression levels. Indeed, IF staining yielded significant LC3 staining by multiple antibodies, as indicated in Table 1 and illustrated in Figure S1. We then tested these same antibodies for immuno-EM on ultrathin cryosections. Cells were fixed with 4% PFA overnight (ON) or with 2% PFA and 0.2% GA for 2–3 h [39], and processed for double-immunogold labeling of LC3B (PAG10) and GFP (PAG15). Remarkably, of the 9 anti-LC3 antibodies tested (Table 1), only the mouse monoclonal Cosmo Bio CAC-CTB-LC3-2-IC anti-LC3B antibody (further referred to as Cosmo Bio anti-LC3B) yielded significant labeling in immuno-EM (Figure 1B, Figure S2F). In heavily overexpressing cells both LC3B and GFP labeling resulted in the presence of gold particles over the cytoplasm and nucleus, as has been reported before [45, 46]. Cells with such a strong label for both LC3B and GFP (indicating high EGFP-LC3B expression) occurred alongside with cells with no label for GFP and little or no label for LC3B, confirming that the Cosmo Bio anti-LC3B specifically

labels LC3B. Under the same conditions, little or no LC3B was detected with any of the other antibodies (Table 1, Figure 1C, Figure S2A-E). Collectively, the data show that a positive result in IF does not guarantee immunogold labeling in immuno-EM. Similar results were recently described in van der Beek et al. [47], in which IF and EM-stained sections were compared directly using correlative light – EM (CLEM). Based on these data we selected the mouse monoclonal Cosmo Bio anti-LC3B for subsequent experiments.

Immuno-EM of endogenous LC3 on ultrathin cryosections

The ultimate goal of this study is to detect endogenous levels of LC3B by immuno-EM. To test the ability of the Cosmo Bio antibody to label endogenous LC3B, we starved U2OS cells in Earle's Balanced Salt Solution (EBSS) for 2.5 h in the presence of BafA1. BafA1 is an inhibitor of the vacuolar type H^+-ATPase (V-ATPase) and causes a pH increase in lysosomes, leading to a decreased degradation capacity [48–51]. Nutrient starvation results in enhanced LC3B levels and an increase in the number of fluorescent LC3B-positive puncta, especially in cells treated with BafA1 when degradation in autolysosomes is abolished [20, 52]. Previous studies reported that starved U2OS cells show a strong increase in autophagy in these conditions, indicating these cells are a suitable model for our studies [52]. When we examined the effect of BafA1 on the morphology of U2OS cells by conventional EM, we indeed found an increase in the number of autophagic compartments, in particular autolysosomes, when compared to control conditions (Figure 2A-B). The autolysosomes in BafA1-treated cells had a typical heterogeneous content with clearly discernable autophagic content (indicated by asterisks in model in Figure 1A and in EM picture in Figure 2B), which accumulates in these conditions due to the block in degradation caused by BafA1.

Most IF studies are performed on permeabilized cells, yielding images of the entire 3D cell volume. Immuno-EM, however, requires the preparation of ultrathin sections. The step from cells (with an average height of 10 µm) to sections

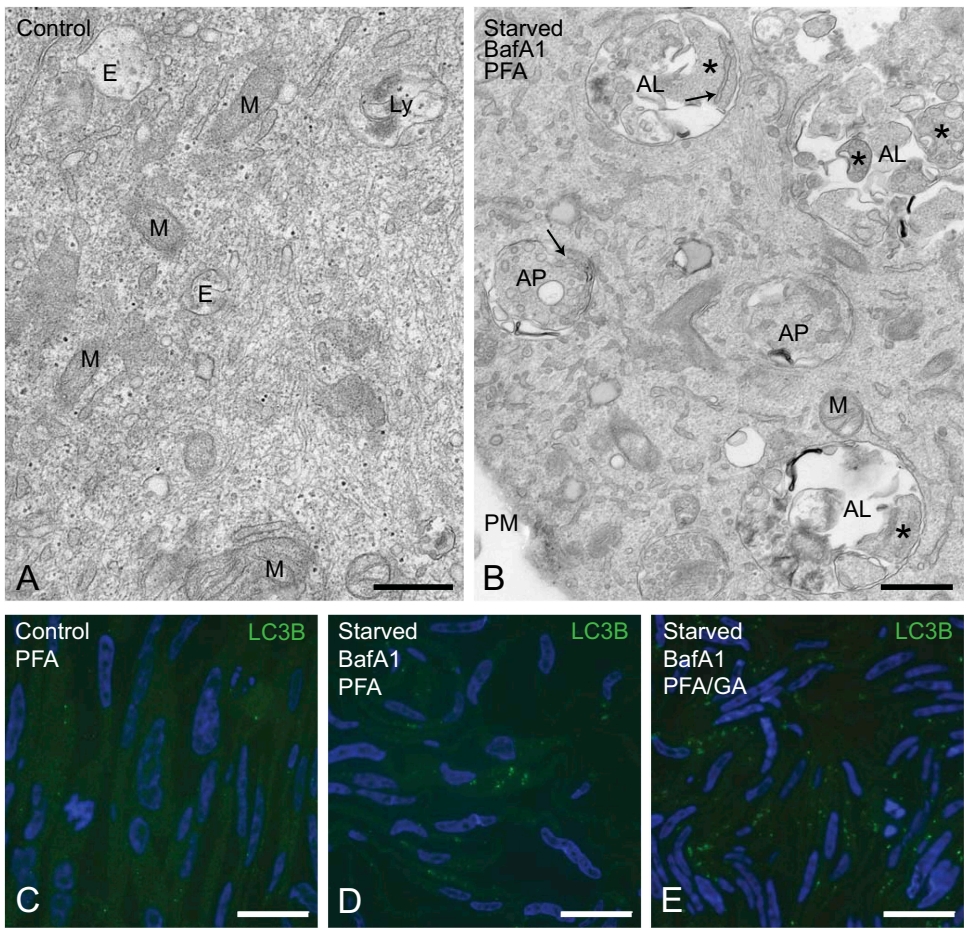

Figure 2. Imaging autophagy by conventional EM and immunofluorescence. (A) Conventional EM of control U2OS cells. Endo-lysosomal compartments are identified by morphology. (B) Conventional EM of U2OS cells starved for 2.5 h in the presence of BafA1 showing an accumulation of different types of autophagic compartments. Autophagosomes (AP) are recognized by their double-membrane that encapsulates part of the cytoplasm with the same density as the surrounding cytoplasm and containing multiple membrane structures. Autolysosomes (AL) are vacuoles lined by a single membrane. Their lumen is heterogenous in content (membranes, vesicles, amorphous material) and electron density (from light to dense). Both AP and AL contain recognizable endoplasmic reticulum (ER) cisternae (arrows). Asterisks indicate autophagic content. (C-E) IF of semi-thin cryosections of control and starved, BafA1-treated U2OS cells, fixed either with 4% PFA ON (PFA) or 2% PFA+0.2% GA for 2 h (PFA+GA) and labeled with Cosmo Bio anti-LC3B (1:10) and Alexa Fluor 488-conjugated goat anti-mouse IgG (1:300). Images are recorded with identical settings and represented with equal intensity ranges. PFA and PFA+GA fixed cells contain comparably intense LC3B puncta. AL, autolysosome; AP, autophagosome; E, endosome; Ly, lysosome; M, mitochondrion; PM, plasma membrane. Scale bars: 500 nm (A-B); 20 µm (C-E).

Table 2. Procedure for immuno-EM of ultrathin cryosections (Tokuyasu method).

1. Fix cells
2. Rinse cells and quench fixative.
3. Scrape cells and centrifuge to a pellet.
4. Embed cells in gelatin.
5. Make blocks of cell pellet in gelatin.
6. Cryoprotect blocks with sucrose.
7. Freeze blocks in liquid nitrogen.
8. Cut ultrathin cryosections
9. Retrieve and thaw sections on sucrose-methylcellulose droplets.
10. Store sections.
11. Immunogold labeling.
12. Contrast and dry sections.

(ranging from 50 to 350 nm) significantly reduces the amount of material available for labeling. We therefore first explored if we could reproduce the characteristic fluorescent LC3 pattern obtained on whole cells by using semi-thin (350 nm) cryosections. Control and starved, BafA1-treated U2OS cells were fixed using two different standard immuno-EM protocols (4% PFA ON or 2% PFA+0.2% GA for 2–3 h) and prepared for cryosectioning according to our standard protocol (Table 2, steps (1)-(7)). Semi-thin cryosections were collected on glass slides, labeled with the Cosmo Bio anti-LC3B followed by Alexa Fluor 488-conjugated rabbit anti-mouse IgG (see Methods) and imaged in a widefield fluorescent microscope. This showed few fluorescent LC3B-positive puncta in control cells (Figure 2C) and a strong increase of LC3B-positive dots in cells that were starved in the presence of BafA1 (Figure 2D, E). The LC3B staining pattern was well visible in both PFA-only as well as PFA+GA fixed cells. These data indicate that the Cosmo Bio anti-LC3B can detect endogenous LC3B by IF of semi-thin cryosections.

Next, we used the Cosmo Bio anti-LC3B on ultrathin (50–80 nm) cryosections. Starved, BafA1-treated U2OS cells were fixed ON with 4% PFA and sections were labeled for LC3B, secondary rabbit-anti-mouse IgG, PAG10, Alexa Fluor 488-donkey anti-rabbit IgG and Hoechst nuclear dye. The best signal-to-background ratio was obtained with a 1:10 dilution of the Cosmo Bio anti-LC3B. The use of fluorescent and gold-labeled secondary antibodies allowed us to directly correlate IF with EM pictures using "on-section" CLEM [47, 53, 54], originally described by Vicidomini *et al.* [55]. Similar to 350 nm sections, we found a punctate fluorescent LC3B staining pattern on the 50–80 nm ultrathin cryosections (Figure 3A). By CLEM, the fluorescent LC3B signal displayed significant and specific overlap with immunogold labeling for LC3B (Figure 3B, C). Within this CLEM experiment we found LC3 puncta representing phagophores (Figure 3D) and autolysosomes (Figure 3E, F). In EM, phagophores are recognizable as discontinuous rings of LC3-positive membranes surrounding a part of the cytoplasm. Interestingly, we found fluorescent and PAG10 LC3B-labeled membranes that appeared in the EM image as a collection of vesicular membrane profiles arranged in a ring with a diameter comparable to autophagosomes (Figure 3D). These may represent LC3B-positive vesicles near the edge of the cup-shaped phagophore or cross-sections of the jagged phagophore edge. The autolysosomes (Figure 3E, F) show similar morphological characteristics as in Epon sections (compare for example Figure 2B with 3E, F). Within autolysosomes, LC3B was mostly associated with clearly visible autophagic material (asterisks in Figure 3E, F).

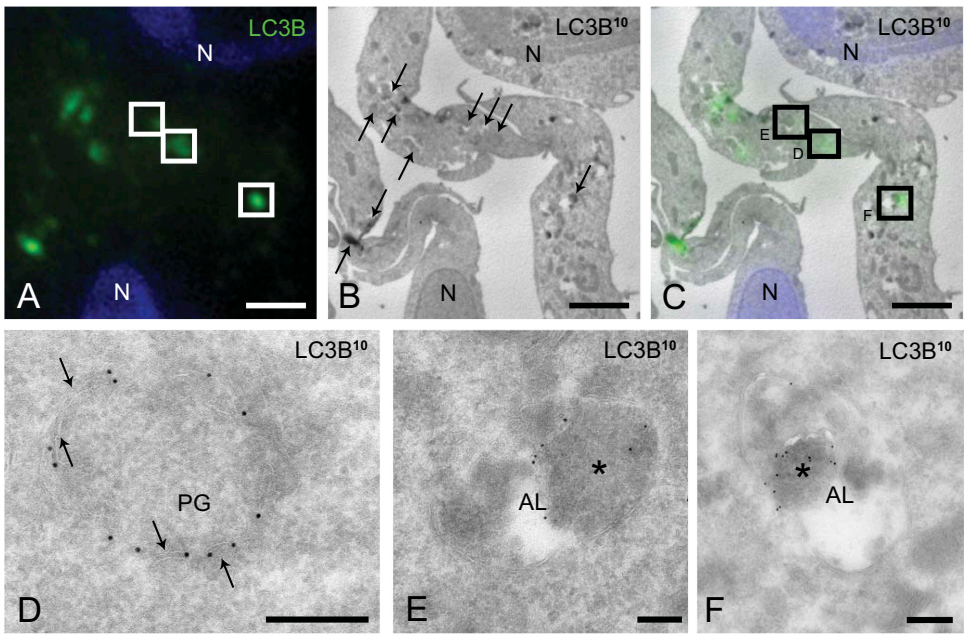

Figure 3. Correlative light electron microscopy (CLEM) of endogenous LC3B on ultrathin cryosections. (A) Ultrathin (60–70 nm) cryosection of starved, BafA1-treated U2OS cells (fixation 4% PFA ON) labeled for LC3B (1:10), rabbit anti-mouse IgG, Alexa Fluor 488-conjugated donkey anti-rabbit IgG and PAG10, showing IF puncta (green) and nuclei (Hoechst, blue). (B) Low magnification EM picture of same section as in (A). Arrows point to LC3B-immunogold labeled compartments (gold not visible at this magnification). (C) Overlay of the fluorescent and EM images in (A) and (B). Higher magnifications of the boxed areas in (C) are shown in (D-F). (D) A phagophore (PG) is visible as a ring of LC3B-positive vesicles. Arrows indicate visible membrane contours. (E, F) Two examples of autolysosomes (AL). LC3B (PAG10) is predominantly associated with autophagic content located in the AL lumen (indicated by asterisks). Note that the higher magnifications in D-F are rotated relative to B. N, nucleus. Scale bars: 2 µm (A-C), 200 nm (D-F).

These findings show that the Cosmo Bio anti-LC3B is suitable for immunolabeling of endogenous LC3B on ultrathin cryosections, either as part of a CLEM approach or directly, by immunogold EM. Using the CLEM approach, we found that the punctate LC3 staining pattern in IF represents distinct autophagy intermediates, which is important to bear in mind when interpreting fluorescent images.

Balancing between labeling yield and morphology

To find the best conditions for optimal LC3-labeling yield while at the same time preserving morphology, we tested the performance of the Cosmo Bio anti-LC3B in several fixation and labeling regimes. In an attempt to reduce the process of membrane extraction, we shortened several steps of the labeling protocol (Table 2 and Materials and Methods, Tokuyasu

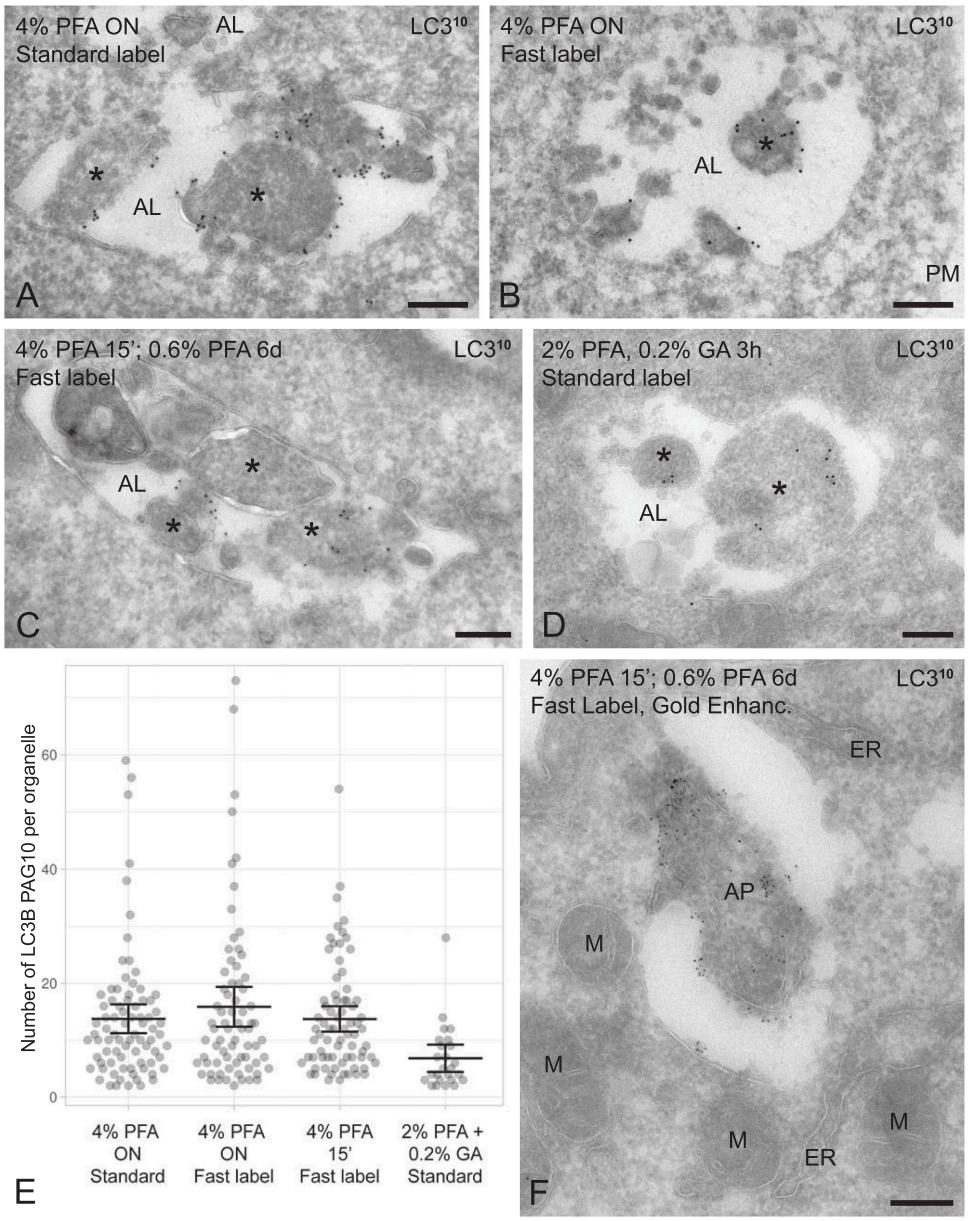

Figure 4. Effect of different fixation and labeling regimes on LC3 immuno-EM labeling efficiency. (A-D) Electron micrographs of U2OS cells starved in the presence of BafA1 for 2.5 h. Cells were fixed and immunolabeled for LC3B (1:10; PAG10) according to the standard or fast labeling protocol as indicated. (A, B) Cells fixed ON with 4% PFA labeled by the standard (A) or fast (B) protocol. Both conditions show abundant LC3B label on autophagic content (asterisks) present in autolysosomes (AL). (C) Cells fixed for 15 min with 4% PFA, followed by 6 days of 0.6% PFA and labeled by the fast protocol. (D) Cells fixed for 3 h with 2% PFA+0.2% GA labeled by the standard protocol. Note a reduction in LC3B label compared to A-C. (E) Quantification of the number of LC3B-representing PAG10 particles per organelle for the conditions shown in A-D. Cells were randomly screened for LC3B-positive organelles. The number of organelles (N) screened was 80, 71, 74 and 25 for conditions indicated in A, B, C and D, respectively. Only the PFA+GA condition significantly differs from the others at $p \leq 0.0001$ using Student's *t*-test assuming unequal variance (***). (F) Starved, BafA1-treated U2OS cells fixed with 4% PFA for 15 min followed by 6 days with 0.6% PFA. Representative image of an autophagosome (AP) labeled for LC3B (1:6) using a gold enhancement step after PAG5 labeling. AP, autophagosome; ER, endoplasmic reticulum; M, mitochondrion. Scale bars: 200 nm.

immuno-EM procedure: steps 10–11) and tested whether this gave an overall increase in LC3 labeling. As illustrated in Figure 4A, B and quantified in Figure 4E, this did not increase LC3B label efficiency. Similar results were obtained when using an alternative fixation protocol (Table 2 in Materials and Methods: step 1) of 4% PFA for 15 min followed by 0.6% PFA for 6 days (Figure 4C, quantified in E). We also found no effect on labeling efficiency or morphology when we used 0.1 M PB or PHEM buffer (data not shown). Adding a low percentage of GA (2% PFA+0.2% GA fixation) generally preserved morphology better over PFA-only fixation, but resulted in less LC3B label (Figure 4D, quantified in E). Despite this, we still obtained a clear signal-to-background ratio, which makes this a feasible fixation protocol for some applications.

As an alternative approach to increase LC3 labeling, we applied gold enhancement combined with the fast-labeling protocol described above (see Materials and Methods for details). In previous studies this has been successfully applied to detect LC3 in a pre-embedding labeling procedure [20,56]. While antibodies can penetrate into a cryosection, the commonly used PAG10 (or PAG15) particles cannot and only bind to antibodies exposed at the section surface. Ultrasmall gold or PAG5 can (partially) penetrate into the section to bind to deeper located antibodies, but need an enhancement step to grow into gold particles readily visible by EM. In Figure 4F we show that the Cosmo Bio anti-LC3B performs very well in the gold enhancement method, resulting in a strong and specific signal for endogenous LC3B. Of note, since the resulting gold size is variable, the labeling obtained with this method is more variable than using PAG and less suited for quantitative studies or double labeling immuno-EM approaches to detect LC3B in direct comparison with other proteins of interest.

We then analyzed the level of morphological preservation using the different PFA-only or PFA+GA fixation regimes described above, combined with PAG10 labeling for LC3. In Figure 5, we show representative EM images of phagophores, autophagosomes and autolysosomes in 4 different conditions, using combinations of different fixations and the standard or fast labeling protocol. In general, the double membrane of phagophores and autophagosomes appears as a halo around the encapsulated cytoplasm (Figures 5A, C, E, G). At the borders of this halo, fragments of the inner (open arrowheads) and outer (closed arrowheads) membrane are visible, with LC3 immunogold label regularly present on both the outer and inner membrane (arrows). Of note, the discontinuity of the phagophore double-membrane may lay outside the plane of the ultrathin section, so they cannot always with certainty be distinguished from autophagosomes. The halo marking phagophores and autophagosomes represents extraction of the double membrane. This is caused by the mild aldehyde fixation used for cryosections, fixing proteins but not lipids, while phagophore and autophagosome membranes are exceptionally low in proteins [44]. In a further attempt to improve morphology, we performed pickup of PFA or PFA+GA fixed sections with methyl-cellulose and 2% uranyl acetate, a method previously used for improved membrane preservation in cryosections [57]. In these conditions, however, the LC3 label was almost extinguished (data not shown). Similar results were found when applying "*en bloc*" uranyl acetate staining of PFA or PFA+GA fixed cells (data not shown). Autolysosomes are well preserved in cryosections and resemble the classical morphology of Epon embedded cells (Figure 2B), appearing as single membrane-bounded vacuoles with a mixed electron-lucent and electron-dense content, sometimes containing numerous small vesicles (Figure 5B, D) or recognizable cytoplasmic content (Figure 5F). LC3 label is mostly concentrated in the autophagic content (asterisks) that accumulates in the lumen of autolysosomes after BafA1 treatment. Little or no LC3 label is present at the limiting membrane. We did not make a distinction between autolysosomes and amphisomes, since both are endo-lysosomal compartments and their morphological differences are not yet clearly defined in literature. In all conditions, we could see the characteristic features of both these early and late stages of autophagy. However, the overall morphology of PFA+GA fixed cells is better and less variable than of PFA-only fixed sections.

Based on these findings we recommend using a 4% PFA fixation in case the most sensitive labeling conditions are required. When the level of LC3B is sufficiently high, a combination fixation of 2% PFA and 0.2% GA can be used, which will lead to overall better morphology. In all conditions, the fast-labeling protocol can be used (Materials and Methods, Tokuyasu immuno-EM procedure, steps 10–11).

Immuno-EM of endogenous LC3B in primary cells and tissues without BafA1 treatment

We next extended our optimized LC3 immuno-EM protocol to primary cells and tissues, derived from mice and rats (Figure 6). Despite the fact that these samples were not treated with BafA1, we found specific endogenous LC3 label, illustrating the robustness of the LC3B immuno-EM signal. Without BafA1, LC3 in autolysosomes is rapidly degraded. Accordingly, the most prevalent LC3-positive structures in these conditions were autophagosomes. Figure 6 shows a collection of labeled autophagosomes in starved mouse macrophages, rat exocrine pancreas and liver hepatocytes. The primary mouse macrophages were fixed with 4% PFA ON or 2% PFA+0.2% GA for 3 h. Both fixations resulted in a significant LC3B immunogold labeling (Figure 6A). and B In agreement with the U2OS EM data, the labeling was highest in PFA-fixed cells (Figure 6A), while macrophages fixed with PFA+GA displayed a better ultrastructure (Figure 6B). Note that also in these cells LC3 label is visible at both the inner and outer autophagosome membrane (arrows). Similar data were obtained when examining ultrathin cryosections of pancreas (Figure 6C-F) and liver (Figure 6G, H) of starved rats. As in cultured cells, the double membrane of autophagosomes appeared with the characteristic white gap (Figure 6D) and LC3 label was present at both the inner and outer autophagosome membrane (Figure 6F, H). These findings show that the Cosmo Bio antibody can be used for immuno-EM of cells or tissues of human as well as murine or rat origin, in the presence or absence of BafA1.

Fusion between autophagosomes and lysosomes continues in the presence of BafA1

An important advantage of PAG-based immuno-EM is that double- and even triple-labeling experiments can be performed

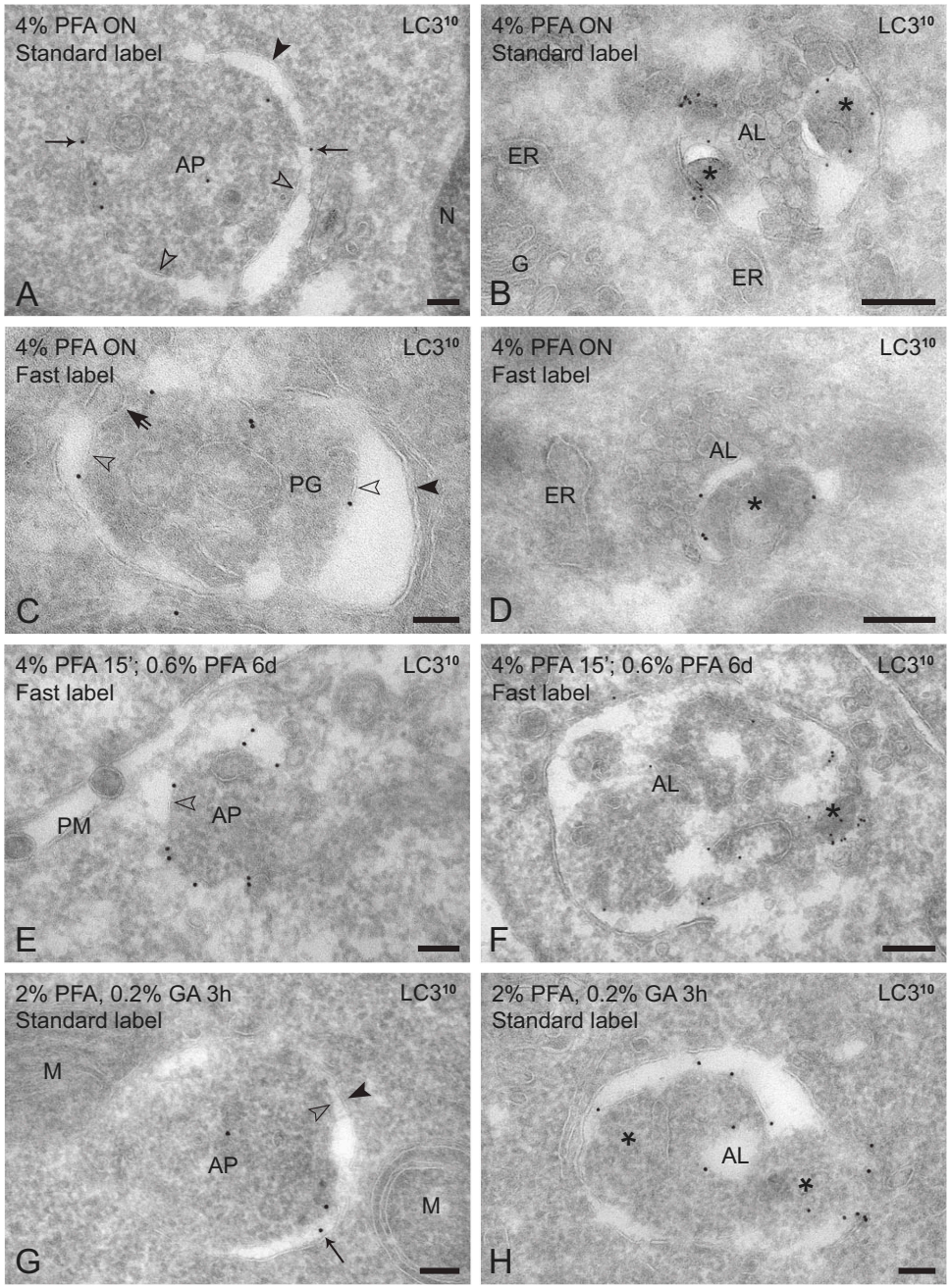

Figure 5. Effect of different fixation and labeling regimes on morphology. U2OS cells starved for 2.5 h in the presence of BafA1, fixed and labeled with Cosmo Bio anti-LC3B and PAG10 according to the indicated fixation and labeling protocols. (**A, E, G**) Typical examples of autophagosomes (AP) using different fixation and labeling regimes. The double membrane is partially extracted resulting in a halo with remnants of inner (open arrowheads) and outer (black arrowheads) membrane. Arrows indicate LC3 PAG10 associated with the outer membrane. (C) Phagophore (PG), recognizable by the edge (shafted arrowhead) of the cup-shaped double membrane. (**B, D, F, H**) Examples of autolysosomes (AL) using the indicated fixation and labeling regimes. Autolysosomes typically contain autophagic content (asterisks) positive for LC3B, are sometimes filled with internal vesicles and display an overall heterogeneous content. The different PFA fixations yield comparable morphologies. The PFA+GA fixation yields an overall better ultrastructure, yet still results in the halo around phagophores and autophagosomes. Dilutions Cosmo Bio LC3B antibody: 1:4 (A, C, D), 1:10 (B, E-H). Asterisk, autophagic content. ER, endoplasmic reticulum; G, Golgi; M, mitochondrion; N, nucleus; PM, plasma membrane. Scale bars: 100 nm (A, C, E, G, H), 200 nm (B, D, F).

by using differentially sized gold particles. As application for this approach, we studied the effects of BafA1 treatment on autolysosome formation. After fusion of an autophagosome and a lysosome, the remaining LC3-labeled inner autophagosomal membrane is rapidly degraded. Hence, LC3-labeled autophagic content only becomes apparent when lysosomal degradation is blocked, e.g. when using BafA1. As shown in Figures 3–5, we regularly found LC3B-labeled autophagic content within autolysosomes of BafA1 treated cells. Studies on the effects of BafA1 on lysosome-autophagosome fusion, however, have yielded conflicting results [50, 51, 58, 59]. For example, Yamamoto et al. [50] and Mauvezin and Neufeld [59] by fluorescence and EM of plastic sections found that autophagosomes and lysosomes remain separated in the presence of BafA1, indicating a block in fusion. In contrast, Fass et al. [51] found GFP-LC3 inside LAMP1-positive vacuoles by IF, suggesting that

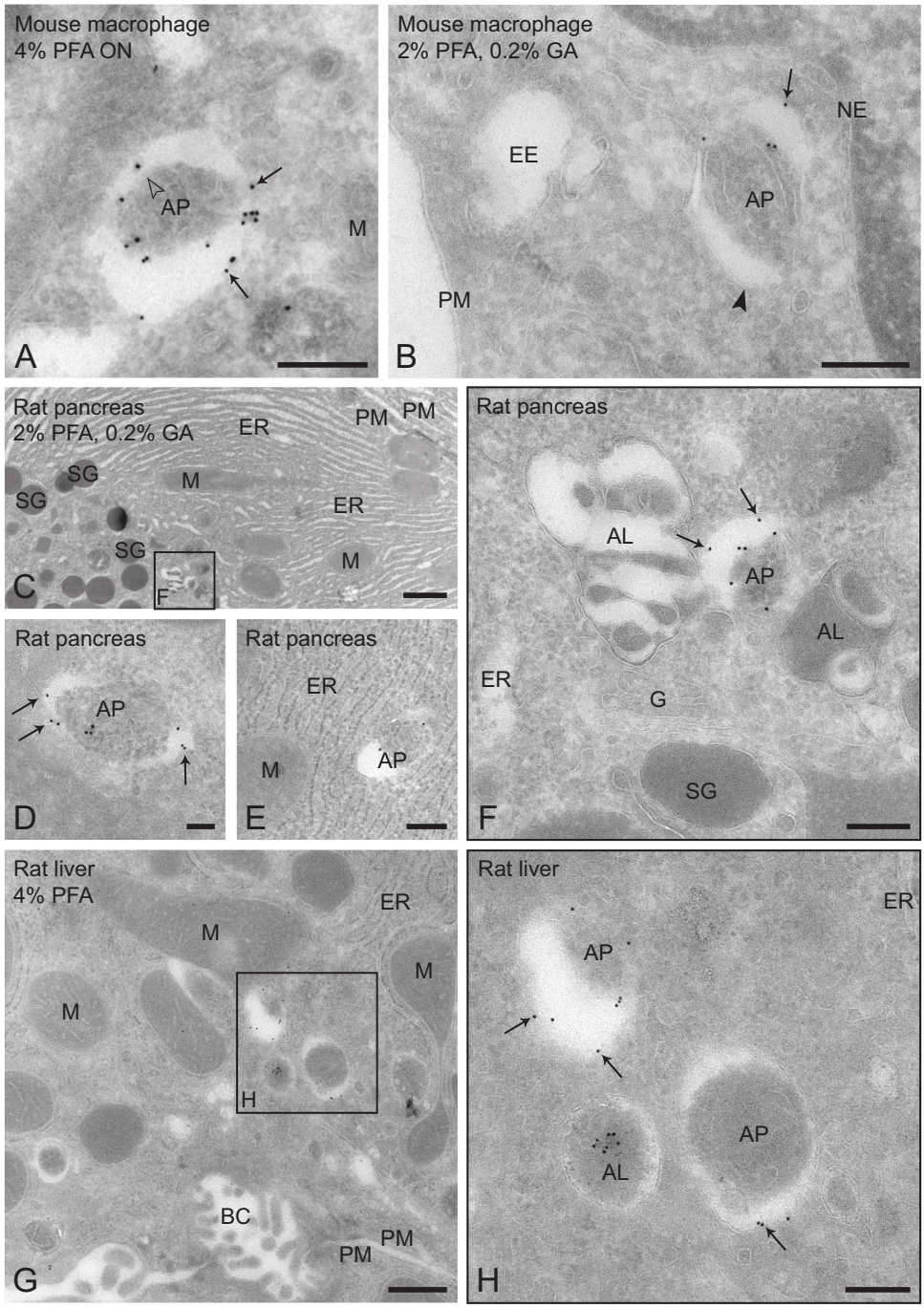

Figure 6. Immuno-EM of endogenous LC3B in primary cells and tissues. (A-B) Primary mouse macrophages were starved for 30 min without addition of BafA1. LC3B labeling (1:6; PAG10, arrows) is detected on autophagosomes (AP) and autolysosomes (AL). Gold particles are associated with the inner (open arrowheads) and outer (black arrowheads) autophagosome membrane. (A) Cells fixed ON with 4% FPA. (B) Cells fixed with 2% PFA+0.2% GA for 2 h. (C-H) In rat pancreas and liver (1:10; PAG10), in the absence of lysosomal inhibitors, LC3B labeling is detected mainly on autophagosomes (AP) and occasionally on an autolysosome (AL). Gold particles are associated with the inner and outer (arrows) autophagosome membrane. (C-F) Rat exocrine pancreas perfusion fixed with 2% PFA+0.2% GA. (C) Overview. (D, E) Examples of autophagosomes (AP) encapsulating mainly ER membranes. (F) Group of 2 (not-labeled) autolysosomes (AL) and an autophagosome (AP) near the Golgi (G), enlarged from the box in (C). LC3 immunogold label is present on inner and outer (arrows) AP membrane. (G, H) Rat liver perfusion fixed with 4% PFA. (H) LC3 immunogold label on a group of autophagosomes (AP) and an autolysosome (AL) in a hepatocyte, enlarged from the box in (G). Arrows indicate LC3 gold on the outer AP membrane. BC, bile canaliculus; EE, early endosome; ER, endoplasmic reticulum; M, mitochondrion; NE, nuclear envelope; PM, plasma membrane; SG, secretory granule. Scale bars: 100 nm (D), 200 nm (A, B, E, F, H), 1 µm (C), 500 nm (G).

fusion of autophagosomes and lysosomes proceeds. To establish the effect of BafA1 on lysosome – autophagosome fusion we designed an experimental setup using 3 different gold sizes. First we incubated U2OS cells with BSA[5] (bovine serum albumin conjugated to 5-nm gold particles), a fluid phase endocytic marker commonly used in EM studies [60–63]. Cells were fixed after a 1.5-h pulse with BSA[5] and 5.5-h chase (Figure 7A), at which time the bulk of BSA[5] is restricted to lysosomes. During the last 2.5 h of the chase, cells were treated with BafA1 and deprived of nutrients. We combined this with

on-section double-labeling for LC3 and the lysosomal membrane protein LAMP1 (PAG10 and PAG15, respectively). Previous studies [64] showed that when autophagosomes fuse with lysosomes, the inner autophagosome membrane and bound LC3 are degraded within less than 10 min. Hence, within our experimental setup the presence of LC3 within BSA^5-marked lysosomes would indicate that autophagosome-lysosome fusion proceeds during the 2.5 h BafA1 treatment.

We prepared the cells for both conventional EM of Epon sections (Figure 7B) and immuno-EM of cryosections (Figure 7C). In both preparation methods BSA^5 was detected (black arrowheads) in compartments with a morphology characteristic for autolysosomes, i.e. a single limiting membrane and a mixture of intraluminal vesicles, dense and lucent amorphous material and autophagic content (indicated by asterisks). Furthermore, by immuno-EM we confirmed the presence of LC3B in autolysosomes that were also positive for BSA^5 (Figure 7C), indicating that fusion between lysosomes (marked by BSA^5) and autophagosomes (marked by LC3B) progresses in the presence of BafA1. To further characterize these BSA^5- and LC3B-positive autolysosomes, we performed double immunogold labeling for the lysosomal membrane protein LAMP1 (PAG10) and LC3B (PAG15). Autolysosomes showed abundant LAMP1 labeling mainly on the limiting membrane and to a lesser extent on internal vesicles (Figure 7D). These data clearly show that after 2.5 h starvation in the presence of BafA1, LC3B

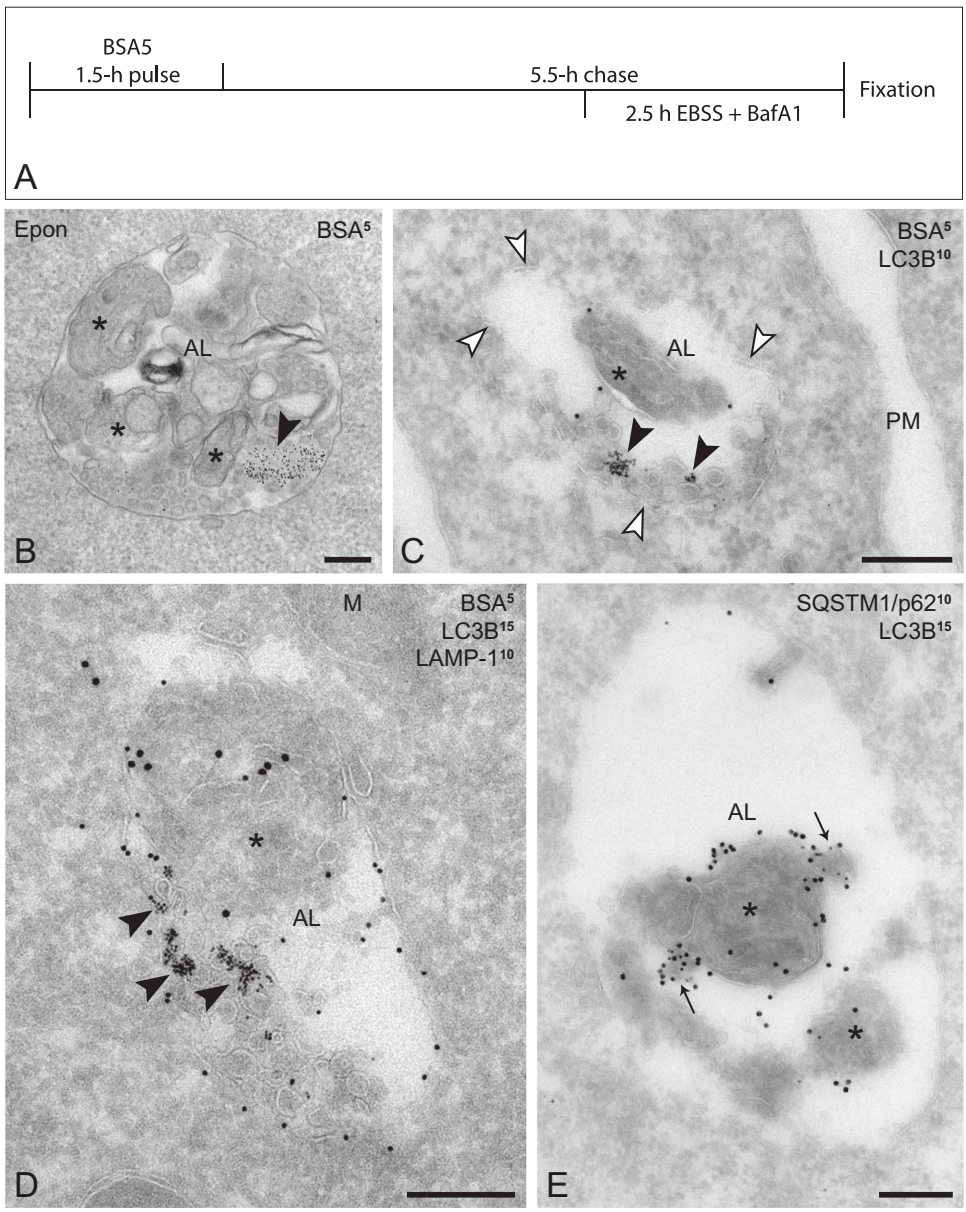

Figure 7. LC3B colocalizes with endocytosed BSA^5, LAMP1 and SQSTM1/p62 in autolysosomes of starved, BafA1-treated U2OS cells. (A) Timeline of experimental setup. (B) Epon section showing BSA^5-containing autolysosome (AL) with similar morphological features as the AL in (C). (C) LC3B (1:4; PAG10) is present in an autolysosome (AL) also containing BSA^5 (black arrowheads). White arrowheads mark the limiting membrane of the AL, showing that LC3B and BSA^5 colocalize in the AL lumen. (D) Double labeling of LAMP1 (1:60; PAG10) and LC3B (1:10; PAG15). Accumulation of LC3B inside a LAMP1-positive autolysosome (AL) also positive for endocytosed BSA^5 (black arrowheads). (E) Colocalization of LC3B (1:6; PAG15) and SQSTM1/p62 (1:100; PAG10) in a typical autolysosome (AL). SQSTM1/p62 label (arrows) marks only a subset of the LC3B-positive material. Fixation for immuno-EM: (C) and (E) 4% PFA ON; (D) 2% PFA, 0.2% GA, 3 h. Asterisks, autophagic content. PM, plasma membrane. Scale bars: 200 nm.

(PAG15) is incorporated into LAMP1-positive (PAG10) autolysosomes that also contain internalized BSA[5].

To add another autophagy protein to these studies, we also performed co-localization of LC3 with SQSTM1/p62. SQSTM1/p62 binds ubiquitinated cytoplasmic proteins destined for degradation to be recruited by membrane-bound LC3s into autophagosomes [65–69]. Previous IF and immuno-EM studies indicated that BafA1 treatment, as for LC3, also results in the accumulation of SQSTM1/p62 [67, 70]. Double-labeling for LC3B (PAG15) and SQSTM1/p62 (PAG10) indeed showed that the two proteins co-localize in autolysosomes of starved, BafA1-treated cells (Figure 7E), providing additional evidence that autophagy proteins enter autolysosomes in the presence of BafA1. Notably, SQSTM1/p62 co-localized only with part of the LC3B-positive content, consistent with the notion that multiple autophagy receptors can mediate LC3-dependent targeting to autolysosomes.

As pointed out in a recent survey on the controversy [14, 58], the discrepancies on the effect of BafA1 on lysosomal fusion may be explained by the duration of BafA1 treatment. To investigate whether longer treatments with BafA1 do inhibit fusion between autophagosomes and lysosomes we treated U2OS cells for 2.5, 5, 10 or 24 h with BafA1 and induced autophagy by starving cells during the last 2.5 h of BafA1 treatment. The extended BafA1 treatment led to a vast increase in the size of (auto)lysosomes (Figure 8A-D, Figure S3), caused by the increase in pH and decreased degradation of internal substrates. For quantification, cryosections were double-labeled for LC3 (PAG15) and LAMP1 (PAG10) and randomly scanned for LC3-positive structures (Figure 8A-D). Each LC3-positive structure was marked as LAMP1-negative (representing phagophores or autophagosomes) or LAMP1-positive (representing amphisomes or autolysosomes). Strikingly, at all time-points, more than 90% of the LC3-positive structures represented autophagic content captured within LAMP1-positive autolysosomes (Figure 8E). At no time-point did we find an accumulation of LC3-positive, LAMP1-negative autophagosomes (Figure 8E). We conclude from these data that 2.5- to 24-h BafA1 treatment prevents degradation (of LC3) in autolysosomes, but does not inhibit fusion between autophagosomes and lysosomes.

Together these data show that in U2OS cells starved in the presence of BafA1, the autophagy proteins LC3B and SQSTM1/p62 are still incorporated into autolysosomes, indicating that autophagosome-lysosome fusion proceeds, even after 24 h BafA1 treatment. Methodologically, these experiments show that our immuno-EM method is compatible with LC3B double labeling and quantitative EM studies, by yielding reproducible and significant label while maintaining sufficiently preserved ultrastructure to recognize distinct autophagic intermediates.

Discussion

The extensive research into the regulation of autophagy and the frequent use of LC3 as marker for autophagic flow warrants an urgent need for tools to localize endogenous LC3 with ultrastructural resolution. Here, we present an optimized procedure to localize endogenous LC3B by immuno-EM, exemplified with high-resolution localization images of endogenous LC3B in different experimental conditions and cell types. Our protocol makes use of ultrathin cryosections and is compatible with the use of PAG as well as with ultrasmall gold and subsequent gold enhancement. We demonstrate that the Cosmo Bio anti-LC3B outperforms other commercial options by its ability to label LC3B by immuno-EM. LC3B can be labeled after fixation with 4% PFA or with 2% PFA +0.2% GA using a standard or fast-labeling protocol. The addition of GA diminishes the labeling, but provides improved cell ultrastructure over PFA alone. The here presented immuno-EM method can detect endogenous LC3 even in the absence of BafA1 and in combination with PAG labeling is highly suitable for double and triple-labeling of LC3B with other relevant proteins. Furthermore, the method can be used in quantitative EM studies. Finally, since cryosections are highly suitable for on-section CLEM, our protocol also provides a powerful tool to bridge fluorescent LC3 localization to EM ultrastructure. These immuno-EM applications of endogenous LC3B labeling can be applied in future studies to provide new ultrastructural insights in autophagy-related processes, such as autophagosome formation and interactions between autophagic and endo-lysosomal compartments.

Previous studies have used ultrathin cryosections to label for endogenous LC3 [40–43], but the poor preservation of phagophore and autophagosomal membranes and the lack of a suitable commercial antibody has hampered broader implementation. The novelty of the present paper is the identification of a commercially available LC3B antibody that works well for labeling ultrathin cryosections and the presentation of optimized protocols to establish the best balance between LC3B labeling yield and ultrastructural preservation. We started our studies by testing a panel of commonly used anti-LC3 antibodies for their performance in IF and application on ultrathin cryosections. Immuno-EM essentially differs from IF in that it requires an electron-dense instead of fluorescent label and makes use of ultrathin sections instead of entire cells. Protocols for IF staining can therefore not be simply transferred to immuno-EM. This is also illustrated in this study; several LC3 antibodies performed well in IF (Figure S1) but failed to yield signal in immuno-EM (Figure S2, Table 1). Likewise, we found that addition of GA to the fixative had little effect on IF staining intensity in sections, whereas the immunogold signal was clearly affected (Figure 2 C-E, Figure 4). We recently obtained similar results when we used CLEM to directly compare the performance of endosomal antibodies in IF and immuno-EM [47]. Together these data show that a positive result in IF does not guarantee successful applications in immuno-EM and that GA fixation differentially affects IF and immunogold labeling. In our hands, only the Cosmo Bio anti-LC3B yielded significant fluorescent and immunogold labeling, making it suitable for both IF and immuno-EM.

We show that the here presented protocol can be used for direct immuno-EM or as part of an on-section CLEM experiment. By on-section CLEM the same section is first viewed in the fluorescence microscope and then transferred to transmission EM for subsequent analysis. Ultrathin cryosections – well-known for their use in immuno-EM – are highly

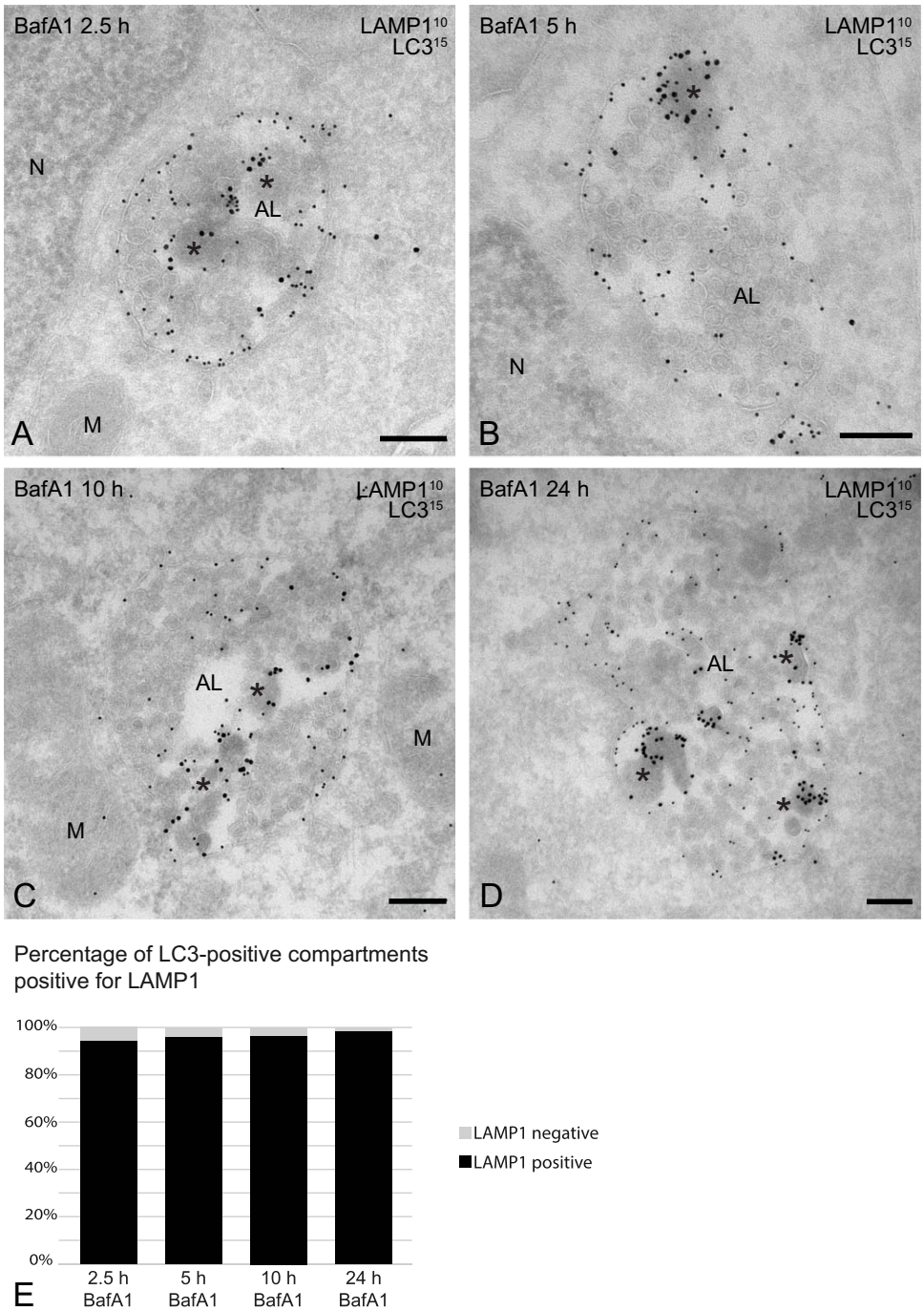

Figure 8. LC3B is incorporated in autolysosomes after extended incubation with BafA1. U2OS cells were treated with BafA1 for the indicated durations and starved in presence of BafA1 using EBSS for 2.5 h before fixation with 4% PFA. Double labeling of LC3B (1:10; PAG15) and LAMP1 (1:100; PAG10) reveals that in all conditions the majority of LC3B label is found in LAMP1-positive autolysosomes (AL). (A) 2.5 h; (B) 5 h; (C) 10 h; (D) 24 h of BafA1 incubation. (E) Quantification of >50 LC3B-positive organelles scored for presence of LAMP1 label per condition. These results indicate that fusion of LC3B-positive autophagosomes with lysosomes proceeds after BafA1 treatment. For more examples of LC3B labeling after BafA1 treatment and the effect on autolysosome morphology, see Fig. S3. Asterisks, autophagic content. M, mitochondrion; N, nucleus. Scale bars: 200 nm.

compatible with IF analysis and on-section CLEM since they do not contain embedding media causing autofluorescence. By marking Cosmo Bio anti-LC3B with both a fluorescent marker and PAG we found a direct correlation between the LC3 fluorescence pattern and the distribution of the correlating gold particles, marking distinct types of autophagic compartments (Figure 3). This CLEM setup thereby improves in accuracy over previous CLEM approaches that were restricted to the use of fluorescent LC3B signal only [71]. Thus, the here presented protocol is well suited for CLEM, which allows one to bridge the data obtained with these two different yet highly complementary imaging technologies. Application of LC3 CLEM may encompass the use of fluorescent images for a quick overview of the number, size, intensity and

distribution of LC3B-positive spots, after which regions of interest can be selected for further examination by EM.

LC3B immuno-EM adds essential information to fluorescence or conventional EM by directly revealing the compartments underlying LC3 staining, at ultrastructural resolution. Furthermore, in combination with the PAG approach immuno-EM can identify the relative distribution of LC3 over (sub-domains of) specified autophagic compartments as well as visualize cellular context, such as the proximity of endosomes, lysosomes, mitochondria, endoplasmic reticulum. Our immuno-EM studies show that fluorescent LC3B spots can represent all stages of autophagy from phagophore to autolysosome. Since the relative distribution of LC3 labeling over distinct autophagic intermediates can differ between cell types and conditions, this heterogeneous distribution should be taken into account during the interpretation of fluorescent LC3 staining patterns. Most LC3B-positive compartments in the starved, BafA1-treated U2OS cells were by EM morphology identified as autolysosomes, which we corroborated by double-labeling with the lysosomal marker LAMP1 and the presence of internalized BSA[5] (Figures 7 and 8). LC3B was found on the peripheral membrane of undegraded autophagic content accumulating inside the autolysosome, illustrating the high level of resolution and context information obtained by immuno-EM.

Autophagosomes were less abundant in BafA1-treated cells and typically appeared as a circular or C-shaped lucent halo, encapsulating part of the cytoplasm. Phagophores were only rarely observed by EM and appeared either as a ring of LC3B-positive vesicular membrane profiles or as C-shaped LC3B-positive cisternae, also often displaying the characteristic halo. The halo represents extraction of the inner and outer phagophore or autophagosome double-membrane, fragments of which are still visible in all conditions we tested. LC3 immunogold label was found on both the inner and outer leaflets of the double-membranes, which confirms early findings of Kabeya et al. by pre-embedding immuno-EM and is in agreement with their biochemical demonstration that pronase treatment of isolated autophagosomes digests about half of the LC3-II content [20]. The extraction of the double membranes is a consequence of the mild aldehyde (PFA+GA) fixation used for cryosections, which fixes proteins but not lipids, while phagophore and autophagosome membranes are exceptionally low in proteins [44]. Previous procedures dedicated to preserve lipids in cryosections included the omission of gelatin embedding to allow preparations fully in the cold, and pickup/thawing of cryosections with 2–3% uranyl acetate as postfixation of the sections [57, 72]. The sensitivity toward uranyl acetate, however, differs between antibodies and unfortunately at concentrations needed to visualize double membranes the LC3 labeling was abolished (data not shown). Though further experimentation with alternative embedding reagents and postfixation methods is possible, these generally have their own drawbacks and limitations. In our experience, the here presented immunogold labeling of cryosections strikes an optimal balance between feasibility, flexibility, preservation of the ultrastructure and labeling efficiency.

Combining LC3 with LAMP1 staining is a powerful approach to discern LAMP1-negative phagophores and autophagosomes from LAMP1-positive amphisomes and autolysosomes. We used this approach to quantitatively assess the presence of LC3 within LAMP1-positive compartments after different time points of BafA1 treatment. Previous studies on the effects of BafA1 yielded conflicting results on whether autophagosome – lysosome fusion is inhibited or proceeds [50, 51, 58, 59]. In recent surveys [14, 58], it was suggested that these discrepancies may be caused by cell-specific effects or by differences in the treatment duration. We show that in the commonly used U2OS cells, when starved for 2.5 h and treated for time intervals of 2.5–24 h with BafA1, fusion between autophagosomes and lysosomes is not inhibited (Figure 8). We found no accumulation of autophagosomes in the cells and in all conditions almost all LC3 label was present on autophagic content within LAMP1-positive autolysosomes. Double labeling of LC3B and SQSTM1/p62 showed that also SQSTM1/p62 accumulates in autolysosomes after BafA1 treatment. Interestingly, SQSTM1/p62 was found only on a limited portion of LC3-positive autophagic content (Figure 7E), illustrating the notion that SQSTM1/p62 labels only a subset of cargoes for autophagy. The SQSTM1/p62 and LC3B double-labeling can hence be used to discern SQSTM1/p62-dependent autophagic cargo recruitment inside autolysosomes. The finding that BafA1 does not block autophagosome-lysosome fusion implies that the vast majority of LC3 puncta seen by IF in BafA1 treated cells represent autolysosomes rather than autophagosomes. This is important for the interpretation of IF images and understanding the block in autophagic flow. Technically, these studies show that our immuno-EM protocol allows to localize LC3 simultaneously with other proteins, has the resolution to discern different subdomains within a single autophagic organelle and is compatible with quantitative EM analyses.

In future studies the here presented immuno-EM procedure for endogenous LC3B labeling can be applied to provide new ultrastructural insights in autophagy-related processes, such as autophagosome formation and interactions between autophagic and endo-lysosomal compartments. To this end, LC3B labeling can be combined with a range of other molecular markers, such as compartmental marker proteins, autophagy machinery or cargoes for selective autophagy, like mitophagy or reticulophagy [73]. During autophagosome formation, for example, membranes from different sources in close contacts are involved [12, 19, 74] and for a full understanding of the process, the precise localization of the LC3-positive membranes among different, closely apposed organelles is a crucial factor. Immuno-EM labeling of endogenous LC3B and double labeling with other proteins of interest can also find applications in non-canonical autophagic processes in which LC3 plays an unconventional role [14, 29]. Among such processes are LC3-associated phagocytosis (LAP) of pathogens and dead cells [75–77], bone resorption in the osteoclast ruffled border [28], lysosomal LC3 lipidation during lysosome repair [22, 23], endosomal microautophagy of LC3 and autophagy receptors [25] and LC3-associated endocytosis (LANDO) [26]. Common to these processes is that some but not all of the autophagic machinery is involved and that LC3B is recruited to single-membrane compartments. The here presented immuno-EM procedure will allow study of these processes at an ultrastructural level without the need for introducing tagged LC3B constructs.

Materials and methods

Equipment

Copper grids (AGAR, AGG2410C); diamond knives Cryo-Immuno 35° for cryo-ultramicrotomy and Ultra 35° for ultramicrotomy (Diatome, "Cryo immuno" and "Ultra 35°"); Ultramicrotomes Reichert Ultracut S (Leica Microsystems) and cryo-ultramicrotomes Leica EM UC6 and UC7 with attached cryo-chamber FC6 and FC7 (Leica Microsystems, Wetzlar, Germany); Transmission electron microscopes JEM-1010 and JEM-1011 (JEOL, Tokyo, Japan), and Tecnai 12 (Thermo Fisher Scientific, MA, USA); fluorescence microscopes Deltavision RT (Applied Precision, Issaquah, WA, USA) and Leica Thunder (Leica Microsystems, Wetzlar, Germany). Formvar- and carbon-coated copper grids were prepared in house (Cell Microscopy Core, University Medical Center Utrecht). Filter paper was from LLG Labware (6.242 668).

Antibodies

The following commercially available antibodies against (human) LC3s were tested: mouse monoclonal anti-LC3B, clone LC3-1703 (Cosmo Bio, CAC-CTB-LC3-2-IC); rabbit anti-LC3A/B (MBL, M152-3); rabbit polyclonal and monoclonal anti-total LC3A/B and rabbit polyclonal anti-LC3B from Cell Signaling Technology (4108, 12741 and 2775, respectively); rabbit polyclonal anti-total LC3A/B from Sigma (L8918); rabbit monoclonal anti-LC3A from Millipore (clone EP1528Y, MABC177); rabbit anti-LC3B (Novus Biologicals, NB600-1384) and mouse anti-LC3B, clone 5F10 (Nanotools, 0231–100/LC3-5 F10). In addition, we used guinea pig anti-SQSTM1/p62 (C terminus) from Progen (GP62-C), rabbit anti-mouse IgG, biotin-conjugated goat anti-GFP and rabbit anti-biotin antibodies from Rockland (610–4120, 600–106-215 and 100–4198, respectively), rabbit anti-GFP, Alexa Fluor 488 PLUS-conjugated goat anti-mouse and donkey anti-rabbit IgG from Thermo Fisher Scientific (A6455, A32723 and A-21206, respectively). For IF on whole cells, we used secondary antibodies Alexa Fluor 568-conjugated rabbit anti-mouse (Life Technologies, A11061) and Alexa Fluor 568-conjugated donkey anti-rabbit (Life Technologies, A10042) IgG. Rabbit anti-LAMP1 [61] was a gift from M Fukuda.

Reagents

Solutions were prepared from the following reagents: PFA prills (Sigma-Aldrich, 441244); GA, EM grade, 8% (wt:vol) in distilled water (Polysciences, 00216); uranyl acetate (SPI-Chem, 02624-AB); methylcellulose, 25 centipoise (Sigma, M-6385); gelatin powder, food quality (Rousselot, 9000–70-8); fish skin gelatin (FSG; Sigma-Aldrich, G7765); acetylated bovine serum albumin (BSA-c; Aurion, 900.022); Gold Enhance EM Plus (Nanoprobes, 2114); Hoechst 33342 (Immunochemistry Technologies, 639); ProLong Diamond Antifade mountant with DAPI (Thermo Fisher Scientific, P36962) and BafA1 (BioAustralis, BIA-B1012). Protein A-gold 1-3-, 5-, 10- and 15-nm particles (PAG1-3, PAG5, PAG10, PAG15), and BSA-gold 5-nm particle (BSA^5) conjugates are made in house (Cell Microscopy Core, UMC Utrecht) [78]. Ten times concentrated phosphate-buffered saline (PBS) stock solution, pH 7.4, was prepared from 2.3 g $NaH_2PO_4.H_2O$, 14.4 g $Na_2HPO_4.2H_2O$, 80 g NaCl and 2 g KCl per liter. 0.2 M Sorensen's phosphate buffer (PB) stock solution, pH 7.4, was prepared from 3.57% $Na_2HPO_4.2H_2O$ and 2.76% $NaH_2PO_4.H_2O$ stock solutions in a 81:19 ratio. Two times concentrated PHEM stock buffer, pH 6.9, consisted of 3.63% PIPES (piperazine-N, N'-bis [2-ethanesulfonic acid] [Merck, 110220]), 1.19% HEPES (Merck, 110110), 0.08% $MgCl_2.6H_2O$, 0.76% EGTA (Sigma-Aldrich, E4378) and NaOH (Merck, 106469) for pH adjustment. Details on the preparation are described in Slot and Geuze [39].

Cells and tissues

U2OS cells (human epithelial osteosarcoma cells, gift from Mario Mauthe, University Medical Center Groningen, Groningen, the Netherlands), were grown to 70% confluency in Dulbecco modified Eagle medium (DMEM; Sigma, D6429-500ML) supplemented with 100 U/ml penicillin, 100 µg/ml streptomycin, and 10% fetal bovine serum (FBS) at 37°C in 5% CO_2 humidified atmosphere. The cells were starved in Earle's Balanced Salt Solution (EBSS; Gibco, 24010–043) for 2.5 h in the presence of 200 nM BafA1. HeLa cells, transiently transfected with EGFP-LC3B, (gift from Dong Yun Lee, Eric Brown Lab, Genentech, USA) were grown in DMEM with 10% FCS, 10 mM HEPES, 100 µM MEM non-essential amino acids (Thermo Fisher, 11140050), 100 U/ml penicillin, 100 µg/ml streptomycin and 0.29 mg/ml-glutamine (Lonza, BE17-605E/U1). Autophagy was induced by starvation in HBSS (Gibco, 14025–050) for 4 h. Mouse bone marrow-derived macrophages (gift from Alex Greer, Eric Brown Lab, Genentech, USA) were cultured in full medium as previously described [79] or starved for 30 min. Liver tissue was obtained from an ON fasted rat, anesthetized with an intraperitoneal injection of Nembutal (90 mg/kg) and perfusion-fixed with 4% PFA in 0.1 M PB. Pancreas tissue was similarly obtained from a rat perfusion-fixed with 2% PFA+0.2% GA in 0.1 M PB.

Immunofluorescence of whole cells on coverslips

For the IF testing of LC3 antibodies, HeLa cells were seeded on coverslips and transfected with plasmid DNA encoding EGFP-LC3B. After 24 h cells were fixed using 4% PFA for 20 min, permeabilized with 0.1% Triton X-100 (Sigma, 9002-93-1) and blocked in 1% BSA (Sigma, Fraction V a4503) in PBS before incubation with the indicated primary antibodies for 1 h in 1% BSA at room temperature (RT). Secondary labeling for 30 min followed, whereafter the coverslips were mounted using ProLong Diamond with DAPI (ThermoFisher, P36962). Fluorescence imaging was performed at RT on a Leica Thunder fluorescence microscope with a 100x, 1.47-NA oil objective, a Photometrics Prime 95B scientific CMOS camera, and LAS X software.

Conventional EM of resin-embedded cells

Cells were fixed with half-strength Karnovsky fixative (2% PFA, 2.5% GA, 0.1 M PB, pH 7.4) for 2 h at RT. After scraping, cells were pelleted and embedded in 2% low melting point agarose. The cell pellets were postfixed as previously described [80] with 1% OsO_4, 1.5% $K_3Fe(CN)_6$, in 0.065 M Na-cacodylate, stained *en bloc* with 0.5% uranyl acetate, dehydrated in acetone and embedded in Epon composed of glycid ether (Serva, 21045.02), 2-dodecenylsuccinic acid anhydride (Serva, 20755.02), methyl nadic anhydride (Serva, 29452.03) and benzyldimethylamine (PolyScience, 00141–100) mixed in weight ratio 48:32:20:3. Ultrathin sections were stained with uranyl acetate and lead citrate.

Tokuyasu immuno-EM procedure

The standard procedure for the preparation of immunogold-labeled cryosections is described in detail by Slot and Geuze [39]. The main steps are listed in Table 2 and briefly described here below.

Main steps of the preparation procedure for immunogold-labeled cryosections for immuno-EM [39]. *At the steps indicated in bold, alternative methods were tested in parallel to the standard procedure in a search for optimal LC3 immuno-EM conditions. These modified preparation steps are described in the text.*

1. Fixation: standard and alternative procedure.

The standard fixations [39] were either 4% PFA ON or 2% PFA+0.2% GA for 2–3 h, both in 0.1 M PB, pH 7.4, or in PHEM, pH 6.9. As an alternative, a drastically milder PFA fixation regimen was applied. A volume of 4% PFA in 0.1 M PB, pH 7, RT, was added to an equal volume of culture medium, swirled gently and left for 5 min. The mixture was replaced by fresh 4% PFA fixative for 10 min at RT. Then fixative was replaced by a storage fixative of 0.6% PFA, 0.1 M PB, and the dishes were sealed with Parafilm and stored at 4°C for 6 days. Animal tissue blocks, obtained after perfusion-fixation with either 4% PFA or 2% PFA+0.2% GA in 0.1 M PB, were postfixed in the same fixative ON or for 2–3 h, respectively.

2. Rinsing and fixative quenching.

Cells and tissue blocks were washed 3 times with PBS, followed by PBS with 0.15% wt:vol glycine for 10 min to quench the fixative.

3. Scraping of cells.

After removal of PBS, 0.15% glycine, the cells were scraped in 1.5 ml of 1% wt:vol gelatin in 0.1 M PB and pelleted in an Eppendorf tube by centrifugation.

4. Embedding of cells and tissue blocks in gelatin.

After replacing the 1% gelatin in 0.1 M PB with 12% wt:vol gelatin in 0.1 M PB at 37°C, the cells were resuspended at 37°C for 10 min and centrifuged. Tissue blocks were gradually embedded in gelatin by incubation in 2%, 6% and 12% gelatin at 37°C. Cell pellets and gelatin-encapsulated tissue blocks were solidified on ice for 30 min.

5. Cutting blocks of gelatin with cells.

The cell pellets were cut to cubic blocks of ~1 mm^3 at 4°C.

6. Cryoprotection of blocks with sucrose.

The blocks of cell pellets or tissue were immersed ON at 4°C in 2.3 M sucrose (VWR, 27483.294) in 0.1 M PB or PHEM buffer.

7. Freezing of blocks in liquid nitrogen.

Blocks were mounted on aluminum specimen holders, frozen and stored in liquid nitrogen.

8. Cutting ultrathin cryosections.

Trimming of the blocks in preparation to thin sectioning was done at −100°C. Ultrathin sections (50–80 nm) were cut at −120°C.

9. Section retrieval and thawing.

Ultrathin sections were picked up with 1.15 M sucrose, 1% methylcellulose droplets [57], thawed and placed at RT on carbon-coated Formvar films on copper grids.

10. Storage of ultrathin cryosections, standard and modified

Storage of freshly cut ultrathin cryosections on grids (Table 2, step 10), routinely 1 to several days, was reduced to a minimum. Immunogold labeling (see 11) was started between 15 min to maximally 2 h after cryosectioning.

11. Immunogold labeling procedure, modified.

As a modification of the standard labeling procedure [39], all rinsing and antibody incubation times were reduced to a minimum. This shortened the procedure for labeling with a single antibody from 190 min in the standard procedure to approximately 140 min.

(1) Place grids, with sections downwards, for 30 min on 35-mm dishes with 3 ml PBS at 37°C to melt and remove the gelatin.

(2) Transfer grids with tweezers to the following series of drops for rinses (200 µl) and incubations (5 µl) on Parafilm adhering to a glass plate.

(3) Wash in PBS, 0.15% glycine, 3 times for 2 min.

(4) Wash in PBS, 0.5% FSG, 0.1% BSA-c, once for 3 min.

(5) Incubate with primary antibody diluted in PBS, 0.5% FSG, 0.1% BSA-c, 30 min.

(6) Wash in PBS, 3 times for 1 min.

(7) In case of rabbit or guinea pig primary antibody, continue with step (10); in case of biotinylated or mouse primary antibody, rinse in PBS, 0.5% FSG, 0.1% BSA-c, 3 min

(8) Incubate with rabbit anti-biotin 1:10,000, or with rabbit anti-mouse IgG, 1:250, in PBS, 0.5% FSG, 0.1% BSA-c, 20 min

(9) Wash with PBS, 3 times for 1 min

(10) Rinse with PBS, 0.5% FSG, 0.1% BSA-c, once for 3 min

(11) Incubate with PAG10 stock solution diluted to an OD_{600} of 0.2 in PBS, 0.5% FSG, 0.1% BSA-c, 20 min

(12) Rinse with PBS, 5 times for 1 min

(13) Stabilize the reaction with 1% GA in PBS, 5 min

(14) For double labeling, repeat steps (3) – (13) with different antibodies and PAG sizes. For the LC3-GFP double labeling, LC3 was first labeled with LC3 antibody, secondary rabbit anti-mouse IgG (in case of a mouse anti-LC3 antibody) and PAG10, followed by GFP labeling either with biotinylated anti-GFP antibody (Rockland), rabbit anti-biotin and PAG15, or with rabbit anti-GFP (Thermo Fisher Scientific) and PAG15. For the LC3-LAMP1 double labeling, LC3 was first labeled with Cosmo Bio anti-LC3B, secondary rabbit anti-mouse IgG and PAG15, followed by rabbit LAMP1 antibody and PAG10. For the LC3-SQSTM1/p62 double labeling,

SQSTM1/p62 was first labeled with the guinea pig anti-SQSTM1/p62 antibody and PAG10, followed by LC3 antibody, secondary rabbit anti-mouse IgG antibody and PAG15. PAG15 is diluted from stock to an OD_{600} of 0.3 in PBS before use.

(15) Wash with double-distilled water, 5 times for 1 min.

12. Contrast and drying.

Float grids on a drop of 2% uranyl oxalate acetate, pH 7, at RT for 5 min, pass them in a few sec over two drops of ice-cold 0.4% uranyl acetate, 1.8% methylcellulose, pH 4, in distilled water and leave them on a third drop of this ice-cold mixture for 5–10 min. Collect grids with a wire loop with an adhering uranyl acetate, methylcellulose droplet and drag the loop in oblique position over a double layer of filter paper to embed the sections in a thin uranyl acetate, methylcellulose film. After 10 min, the grids are sufficiently dry for inspection in the electron microscope.

Quantifications

For Figure 4, numbers of LC3 immunogold particles per autophagic compartment were quantified in randomly sampled sections of cells prepared according to the different fixation and labeling conditions as indicated in Figure 4. Differences in labeling efficiencies were determined by means of Student's *t*-test for unequal variances and graphically represented using the PlotsOfData web app [81].

In the BafA1 time series of Figure 8, for each time point at least 50 LC3-positive compartments were randomly sampled by systematic screening of sections double labeled for LC3 (PAG15) and LAMP1 (PAG10) and scored for the presence of LAMP1 label. Compartments were considered as LC3- or LAMP1-positive if at least 2 gold particles of the respective size were present.

Immunofluorescent detection of endogenous LC3 using semi-thin cryosections

For IF microscopy, we took the frozen blocks with cell pellets from step 7 and made 350 nm thick sections using a glass knife on an ultracryomicrotome at −100°C. Sections were picked up in a loop with a droplet of 1.15 M sucrose, 1% methylcellulose, 0.1 M PB, thawed and placed on 10 mm diameter squeaky-clean coverslips and immediately immunolabeled. For immunolabeling, sections on coverslips were passed face down over 50 µl drops. The labeling was performed by following steps (3) – (9) of the immunolabeling procedure for EM (see step 11), using Alexa Fluor 488 PLUS-conjugated goat anti-mouse IgG, 1:300, as secondary antibody. After final washing with distilled water twice for 3 min, the sections were included between coverslips and object slides with 3 µl Prolong Diamond with DAPI. After drying at RT in the dark for 2 h, the preparations were stored in the dark at 4°C until examination at RT on a Leica Thunder fluorescence microscope with a 100x, 1.47-NA oil objective, a Photometrics Prime 95B scientific CMOS camera, and LAS X software.

Gold enhancement of LC3B immunogold labeled ultrathin sections

The modified immunogold labeling procedure (see step 11) was performed up to the step of the PAG incubation and then continued with the following incubations. The grids were (1) incubated with PAG1-3 or PAG5 solution at an OD_{600} of 0.2, in PBS, 0.5% FSG, 0.1% BSA-c; (2) rinsed with PBS, 5 times for 1 min; (3) fixed with 1% GA in PBS for 3 min; (4) rinsed thoroughly with double-distilled water, 8 times for 2 min; (5); incubated on 40 µl droplets of the gold enhancement mixture prepared following the manufacturer's instructions at RT for 2 min to obtain the desired (± 10 nm) gold particle size; (6) washed 30 sec with 2% sodium thiosulfate to stop the reaction; (7) washed 5 times for 2 min in distilled water; (8) contrasted and dried as done in step 12.

Correlative light and electron microscopy on sections

We used an adapted protocol [47] from Vicidomini et al. [55]. Briefly, ultrathin cryosections of U2OS cells were prepared, placed on grids, and immunogold labeled with the mouse Cosmo Bio anti-LC3B followed by rabbit anti-mouse IgG and PAG10 as described (see immunogold labeling procedure, (1) to (13). Next, the following steps were performed: sections on grids were (1) rinsed in PBS, 0.15% glycine, 3 times for 2 min; (2) rinsed in PBS, 1% FSG, 0.2% BSA-c, 5 min; (3) incubated with Alexa Fluor 488-conjugated donkey anti-rabbit IgG 1:300, in PBS, 1% FSG, 0.2% BSA-c for 20 min; (4) washed with PBS, 3 times for 2 min; (5) incubated with Hoechst 33342, 1:200 in PBS for 20 min; (6) rinsed in PBS, 2 min; (7) rinsed in distilled water, 3 times for 2 min; (8) mounted by dipping the grid in 50% glycerol, placing it with sections facing up on an object slide, and covering it with a coverslip; (9) imaged on a DeltaVision microscope with EMCCD camera at RT; (10) stripped of oil and coverslip; (11) unmounted in distilled water; (12) dried on the back side with filter paper; (13) rinsed on distilled water droplets, 7 times 2 min; (14) contrasted and dried as described above (Tokuyasu immuno-EM procedure, step 12). Images from EM and LM were overlaid in Adobe Photoshop using nuclei as reference points.

BafA1 treatment and BSA^5 uptake

U2OS cells were treated for 2.5, 5, 10 or 24 h with 200 nM BafA1 in the culture medium. Starvation was induced by changing the culture medium to EBSS in the last 2.5 h of BafA1 treatment. In an additional experiment, 2.5 h BafA1 treatment was combined with addition of the endocytic marker BSA^5 using a pulse-chase protocol. Stock solution of BSA^5 was dialyzed ON in a Slide-A-Lyzer cassette (Thermo Fisher Scientific, 66383) in PBS to remove NaN_3 and diluted to an OD_{600} of 4–4.5 in DMEM. The BSA^5 solution was applied to U2OS cells for 1.5 h, followed by a short rinse with DMEM and a chase of 5.5 h. During the last 2.5 h of the 5.5 h chase, the cells were starved by switching from DMEM to EBSS in the presence of 200 nM BafA1 and subsequently fixed.

Abbreviations

BafA1: bafilomycin A_1; BSA: bovine serum albumin; BSA-c: acetylated BSA; BSA^5: BSA conjugated to 5-nm gold particles; CLEM: correlative light-electron microscopy; EGFP: enhanced green fluorescent protein; EM: electron microscopy; FBS: fetal bovine serum; FSG: fish skin gelatin; GA: glutaraldehyde; IF: immunofluorescence; LAMP1: lysosomal associated membrane protein 1; LC3s: LC3 proteins; MAP1LC3/LC3: microtubule associated protein 1 light chain 3; ON: overnight; PAG: protein A-conjugated gold particles; PAG1-3: PAG5, PAG10, PAG15, protein A conjugated to 1-3-, 5-, 10-, or 15-nm gold particles; PB: Sorensen's phosphate buffer; PBS: phosphate-buffered saline; PFA: paraformaldehyde; RT: room temperature.

Acknowledgments

We are grateful to Mario Mauthe (Reggiori lab, UMC Groningen) for valuable discussions and the U2OS cell culture, for which we also thank Martijn Vromans (Lens lab, UMC Utrecht). We thank Dong Yun Lee and Alex Greer from the Eric Brown Lab (Genentech, San Francisco), for providing EGFP-LC3B transfected HeLa cells and mouse bone marrow derived macrophages, respectively. We thank René Scriwanek for excellent assistance with photography and figure lay-out. We thank our colleagues in the Center for Molecular Medicine and especially the Klumperman lab for fruitful discussions and feedback. This work was supported in part by Scientific Research on Innovative Areas (Grant Numbers 26111519, 15H01388 for Masato Koike), Grants-in-Aid for Scientific Research (C) (Grant Numbers 25460276, 17K08522 for Masato Koike), and the Private University Research Branding Project (Masato Koike) from the Ministry of Education, Culture, Sports, Science and Technology of Japan. The electron microscopy infrastructure used for this work is part of the research program National Roadmap for Large-Scale Research Infrastructure (NEMI) financed by the Dutch Research Council (NWO), project number 184.034.014 to JK. ADM and SvD are appointed on Genentech contract 55963 (Intracellular trafficking of tumor antigens and their binding antibodies) to JK.

Disclosure statement

No potential conflict of interest is reported by the authors.

Funding

This work was supported by Genentech [55963]; Japan Society for the Promotion of Science [15H01388]; Japan Society for the Promotion of Science [25460276]; Japan Society for the Promotion of Science [26111519]; Japan Society for the Promotion of Science [17K08522]; Private University Research Branding Project from Ministry of Education, Culture, Sports, Science and Technology of Japan; Nederlandse Organisatie voor Wetenschappelijk Onderzoek [184.034.014].

ORCID

Ann De Mazière http://orcid.org/0000-0001-8070-5104
Jan van der Beek http://orcid.org/0000-0003-4957-9175
Cecilia de Heus http://orcid.org/0000-0001-8618-8451
Fulvio Reggiori http://orcid.org/0000-0003-2652-2686
Masato Koike http://orcid.org/0000-0002-3174-5684
Judith Klumperman http://orcid.org/0000-0003-4835-6228

References

[1] Yang Z, Klionsky DJ. Mammalian autophagy: core molecular machinery and signaling regulation. Curr Opin Cell Biol. 2010;22:124–131.
[2] Mizushima N, Yoshimori T, Ohsumi Y. The role of atg proteins in autophagosome formation. Annu Rev Cell Dev Biol. 2011;27(1):107–132.
[3] Mizushima N, Komatsu M. Autophagy: renovation of cells and tissues. Cell. 2011;147:728–741.
[4] Rubinsztein DC, Shpilka T, Elazar Z. Mechanisms of autophagosome biogenesis. Curr Biol. 2012;22:R29–R34.
[5] Choi AMK, Ryter SW, Levine B. Autophagy in human health and disease. N Engl J Med. 2013;368:651–662.
[6] Shen HM, Mizushima N. At the end of the autophagic road: an emerging understanding of lysosomal functions in autophagy. Trends Biochem Sci. 2014;39:61–71.
[7] Sica V, Galluzzi L, Bravo-San Pedro JM, et al. Organelle-Specific initiation of autophagy. Mol Cell. 2015;59:522–539.
[8] Reggiori F, Ungermann C. Autophagosome maturation and fusion. J Mol Biol. 2017;429:486–496.
[9] Eskelinen EL. Maturation of autophagic vacuoles in mammalian cells. Autophagy. 2006;1:1–10. July 29.
[10] Lamb CA, Yoshimori T, Tooze SA. The autophagosome: origins unknown, biogenesis complex. Nat Rev Mol Cell Biol. 2013;14:759–774.
[11] Nakatogawa H. Mechanisms governing autophagosome biogenesis. Nat Rev Mol Cell Biol. 2020;21:439–458.
[12] Axe EL, Walker SA, Manifava M, et al. Autophagosome formation from membrane compartments enriched in phosphatidylinositol 3-phosphate and dynamically connected to the endoplasmic reticulum. J Cell Biol. 2008;182:685–701.
[13] Li W, He P, Huang Y, et al. Selective autophagy of intracellular organelles: recent research advances. Theranostics. 2020;11:222–256.
[14] Klionsky DJ, Abdel-Aziz AK, Abdelfatah S, et al. Guidelines for the use and interpretation of assays for monitoring autophagy. Autophagy. 2021;17:1–382. 4th edition.
[15] Kuma A, Matsui M, Mizushima N. LC3, an autophagosome marker, can be incorporated into protein aggregates independent of autophagy: caution in the interpretation of LC3 localization. Autophagy. 2007;3:323–328.
[16] Martinet W, Schrijvers DM, Timmermans JP, et al. Immunohistochemical analysis of macroautophagy: recommendations and limitations. Autophagy. 2013;9:386–402.
[17] Rosenfeldt MT, Nixon C, Liu E, et al. Analysis of macroautophagy by immunohistochemistry. Autophagy. 2012;8:963–969.
[18] Mauthe M, Orhon I, Rocchi C, et al. Chloroquine inhibits autophagic flux by decreasing autophagosome-lysosome fusion. Autophagy. 2018;14:1435–1455.
[19] Puri C, Vicinanza M, Ashkenazi A, et al. The RAB11A-Positive compartment is a primary platform for autophagosome assembly mediated by WIPI2 recognition of PI3P-RAB11A. Dev Cell. 2018;45:114–131.e8.
[20] Kabeya Y, Mizushima N, Ueno T, et al. LC3, a mammalian homologue of yeast Apg8p, is localized in autophagosome membranes after processing. EMBO J. 2000;19:5720–5728.
[21] Koike M, Shibata M, Waguri S, et al. Participation of autophagy in storage of lysosomes in neurons from mouse models of neuronal ceroid-lipofuscinoses (Batten disease). Am J Pathol. 2005;167:1713–1728.
[22] Lee C, Lamech L, Johns E, et al. Selective lysosome membrane turnover is induced by nutrient starvation. Dev Cell. 2020;55:289–297.e4.
[23] Nakamura S, Shigeyama S, Minami S, et al. LC3 lipidation is essential for TFEB activation during the lysosomal damage response to kidney injury. Nat Cell Biol. 2020;22:1252–1263.
[24] Florey O, Gammoh N, Kim SE, et al. V-ATPase and osmotic imbalances activate endolysosomal LC3 lipidation. Autophagy. 2015;11:88–99.
[25] Mejlvang J, Olsvik H, Svenning S, et al. Starvation induces rapid degradation of selective autophagy receptors by endosomal microautophagy. J Cell Biol. 2018;217:3640–3655.
[26] Heckmann BL, Teubner BJW, Tummers B, et al. LC3-Associated endocytosis facilitates β-Amyloid clearance and mitigates neurodegeneration in murine alzheimer's disease. Cell. 2019;178:536–551.e14.

[27] Shibata M, Yoshimura K, Tamura H, et al. LC3, a microtubule-associated protein1A/B light chain3, is involved in cytoplasmic lipid droplet formation. Biochem Biophys Res Commun. 2010;393:274–279.
[28] DeSelm CJ, Miller BC, Zou W, et al. Autophagy proteins regulate the secretory component of osteoclastic bone resorption. Dev Cell. 2011;21:966–974.
[29] Bestebroer J, V'kovski P, Mauthe M, et al. Hidden behind autophagy: the unconventional roles of ATG proteins. Traffic. 2013;14:1029–1041.
[30] Eskelinen EL, Reggiori F, Baba M, et al. Seeing is believing: the impact of electron microscopy on autophagy research. Autophagy. 2011;7:935–956.
[31] Eskelinen EL. To be or not to be? Examples of incorrect identification of autophagic compartments in conventional transmission electron microscopy of mammalian cells. Autophagy. 2008;4:257–260.
[32] Biazik J, Ylä-Anttila P, Vihinen H, et al. Ultrastructural relationship of the phagophore with surrounding organelles. Autophagy. 2015;11:439–451.
[33] Kishi-Itakura C, Ktistakis NT, Buss F. Ultrastructural insights into pathogen clearance by autophagy. Traffic. 2020;21:310–323.
[34] Asanuma K, Tanida I, Shirato I, et al. MAP-LC3, a promising autophagosomal marker, is processed during the differentiation and recovery of podocytes from PAN nephrosis. FASEB J. 2003;17:1165–1167.
[35] English L, Chemali M, Duron J, et al. Autophagy enhances the presentation of endogenous viral antigens on MHC class I molecules during HSV-1 infection. Nat Immunol. 2009;10:480–487.
[36] Fine KL, Metcalfe MG, White E, et al. Involvement of the autophagy pathway in trafficking of mycobacterium tuberculosis bacilli through cultured human type II epithelial cells. Cell Microbiol. 2012;14:1402–1414.
[37] Tokuyasu KT. A technique for ultracryotomy of cell suspensions and tissues. J Cell Biol. 1973;57:551–565.
[38] Tokuyasu KT. A study of positive staining of ultrathin frozen sections. J Ultrastruct Res. 1978;63:287–307.
[39] Slot JW, Geuze HJ. Cryosectioning and immunolabeling. Nat Protoc. 2007;2:2480–2491.
[40] Eskelinen E-L, Prescott AR, Cooper J, et al. Inhibition of autophagy in mitotic animal cells. Traffic. 2002;3:878–893.
[41] Jäger S, Bucci C, Tanida I, et al. Role for Rab7 in maturation of late autophagic vacuoles. J Cell Sci. 2004;117:4837–4848.
[42] Köchl R, Hu XW, Chan EYW, et al. Microtubules facilitate autophagosome formation and fusion of autophagosomes with endosomes. Traffic. 2006;7:129–145.
[43] Patel KK, Miyoshi H, Beatty WL, et al. Autophagy proteins control goblet cell function by potentiating reactive oxygen species production. EMBO J. 2013;32:3130–3144.
[44] Fengsrud M, Erichsen ES, Berg TO, et al. Ultrastructural characterization of the delimiting membranes of isolated autophagosomes and amphisomes by freeze-fracture electron microscopy. Eur J Cell Biol. 2000;79:871–882.
[45] Drake KR, Kang M, Kenworthy AK. Nucleocytoplasmic distribution and dynamics of the autophagosome marker EGFP-LC3. PLoS One. 2010;5:e9806.
[46] Huang R, Xu Y, Wan W, et al. Deacetylation of nuclear LC3 drives autophagy initiation under starvation. Mol Cell. 2015;57:456–466.
[47] van der Beek J, de Heus C, Liv N, et al. Quantitative correlative microscopy reveals the ultrastructural distribution of endogenous endosomal proteins. J Cell Biol. 2022;221(1):e202106044.
[48] Bowman EJ, Siebers A, Altendorf KB. A class of inhibitors of membrane ATPases from microorganisms, animal cells, and plant cells. Proc Natl Acad Sci U S A. 1988;85:7972–7976.
[49] Yoshimori T, Yamamoto A, Moriyama Y, et al. Bafilomycin A1, a specific inhibitor of vacuolar-type H+-ATPase, inhibits acidification and protein degradation in lysosomes of cultured cells. J Biol Chem. 1991;266:17707–17712.
[50] Yamamoto A, Tagawa Y, Yoshimori T, et al. Bafilomycin A1 prevents maturation of autophagic vacuoles by inhibiting fusion between autophagosomes and lysosomes in rat hepatoma cell line, H-4-II-E cells. Cell Struct Funct. 1998;23:33–42.
[51] Fass E, Shvets E, Degani I, et al. Microtubules support production of starvation-induced autophagosomes but not their targeting and fusion with lysosomes. J Biol Chem. 2006;281:36303–36316.
[52] Mauthe M, Jacob A, Freiberger S, et al. Resveratrol-mediated autophagy requires WIPI-1-regulated LC3 lipidation in the absence of induced phagophore formation. Autophagy. 2011;7:1448–1461.
[53] Hassink G, Slotman J, Oorschot V, Van Der Reijden B A, Monteferrario D, Noordermeer S M, Van Kerkhof P, Klumperman J, Strous G J. Identification of the ubiquitin ligase Triad1 as a regulator of endosomal transport. Biology Open. 2012;1(6):607–614.
[54] Fokkema J, Fermie J, Liv N, et al. Fluorescently labelled silica coated gold nanoparticles as fiducial markers for correlative light and electron microscopy. Sci Rep. 2018;8:13625.
[55] Vicidomini G, Gagliani MC, Cortese K, et al. A novel approach for correlative light electron microscopy analysis. Microsc Res Tech. 2010;73:215–224.
[56] Mattoscio D, Casadio C, Miccolo C, et al. Autophagy regulates UBC9 levels during viral-mediated tumorigenesis. PLoS Pathog. 2017;13:e1006262.
[57] Liou W, Geuze HJ, Slot JW. Improving structural integrity of cryosections for immunogold labeling. Histochem Cell Biol. 1996;106:41–58.
[58] Klionsky DJ, Elazar Z, Seglen PO, et al. Does bafilomycin A1 block the fusion of autophagosomes with lysosomes? Autophagy. 2008;4:849–850.
[59] Mauvezin C, Neufeld TP. Bafilomycin A1 disrupts autophagic flux by inhibiting both V-ATPase-dependent acidification and Ca-P60A/SERCA-dependent autophagosome-lysosome fusion. Autophagy. 2015;11:1437–1438.
[60] Pols MS, ten Brink C, Gosavi P, et al. The HOPS proteins hVps41 and hVps39 are required for homotypic and heterotypic late endosome fusion. Traffic. 2013;14:219–232.
[61] Pols MS, van Meel E, Oorschot V, et al. hVps41 and VAMP7 function in direct TGN to late endosome transport of lysosomal membrane proteins. Nat Commun. 2013;4:1361.
[62] Galmes R, ten Brink C, Oorschot V, et al. Vps33B is required for delivery of endocytosed cargo to lysosomes. Traffic. 2015;16:1288–1305.
[63] Jonker CTH, Galmes R, Veenendaal T, et al. Vps3 and Vps8 control integrin trafficking from early to recycling endosomes and regulate integrin-dependent functions. Nat Commun. 2018;9:792.
[64] Tsuboyama K, Koyama-Honda I, Sakamaki Y, et al. The ATG conjugation systems are important for degradation of the inner autophagosomal membrane. Science. 2016;354:1036–1041.
[65] Bjørkøy G, Lamark T, Brech A, et al. p62/SQSTM1 forms protein aggregates degraded by autophagy and has a protective effect on huntingtin-induced cell death. J Cell Biol. 2005;171:603–614.
[66] Shvets E, Fass E, Scherz-Shouval R, et al. The N-terminus and Phe52 residue of LC3 recruit p62/SQSTM1 into autophagosomes. J Cell Sci. 2008;121:2685–2695.
[67] Pankiv S, Clausen TH, Lamark T, et al. p62/SQSTM1 binds directly to Atg8/LC3 to facilitate degradation of ubiquitinated protein aggregates by autophagy. J Biol Chem. 2007;282:24131–24145.
[68] Berkamp S, Mostafavi S, Sachse C. Structure and function of p62/SQSTM1 in the emerging framework of phase separation. FEBS J. 2021;288:6927–6941.
[69] Anding AL, Baehrecke EH. Cleaning house: selective autophagy of organelles. Dev Cell. 2017;41:10–22.
[70] Shvets E, Elazar Z. Autophagy-independent incorporation of GFP-LC3 into protein aggregates is dependent on its interaction with p62/SQSTM1. Autophagy. 2008;4:1054–1056.
[71] Zhen Y, Spangenberg H, Munson MJ, et al. ESCRT-mediated phagophore sealing during mitophagy. Autophagy. 2020;16:826–841.

[72] Liou W, Geuze H J, Geelen M JH, Slot J W. The Autophagic and Endocytic Pathways Converge at the Nascent Autophagic Vacuoles. Journal of Cell Biology. 1997;136(1):61–70.
[73] Khaminets A, Heinrich T, Mari M, et al. Regulation of endoplasmic reticulum turnover by selective autophagy. Nature. 2015;522:354–358.
[74] Puri C, Renna M, Bento CF, et al. Diverse autophagosome membrane sources coalesce in recycling endosomes. Cell. 2013;154:1285–1299.
[75] Martinez J, Almendinger J, Oberst A, et al. Microtubule-associated protein 1 light chain 3 alpha (LC3)-associated phagocytosis is required for the efficient clearance of dead cells. Proc Natl Acad Sci U S A. 2011;108:17396–17401.
[76] Heckmann BL, Green DR. LC3-associated phagocytosis at a glance. J Cell Sci. 2019;132:jcs222984.
[77] Herb M, Gluschko A, Schramm M. LC3-associated phagocytosis - The highway to hell for phagocytosed microbes. Semin Cell Dev Biol. 2020;101:68–76.
[78] Slot JW, Geuze HJ. A new method of preparing gold probes for multiple-labeling cytochemistry. Eur J Cell Biol. 1985;38:87–93.
[79] Roach TIA, Slater SE, White LS, et al. The protein tyrosine phosphatase SHP-1 regulates integrin-mediated adhesion of macrophages. Curr Biol. 1998;8:1035–1039.
[80] Collins CA, De Mazière A, van Dijk S, et al. Atg5-independent sequestration of ubiquitinated mycobacteria. PLoS Pathog. 2009;5:e1000430.
[81] Postma M, Goedhart J. PlotsOfData-A web app for visualizing data together with their summaries. PLoS Biol. 2019;17:e3000202.